



Regular / Irregular Climate Changes and Uncertainties

VAROTSOS Costas

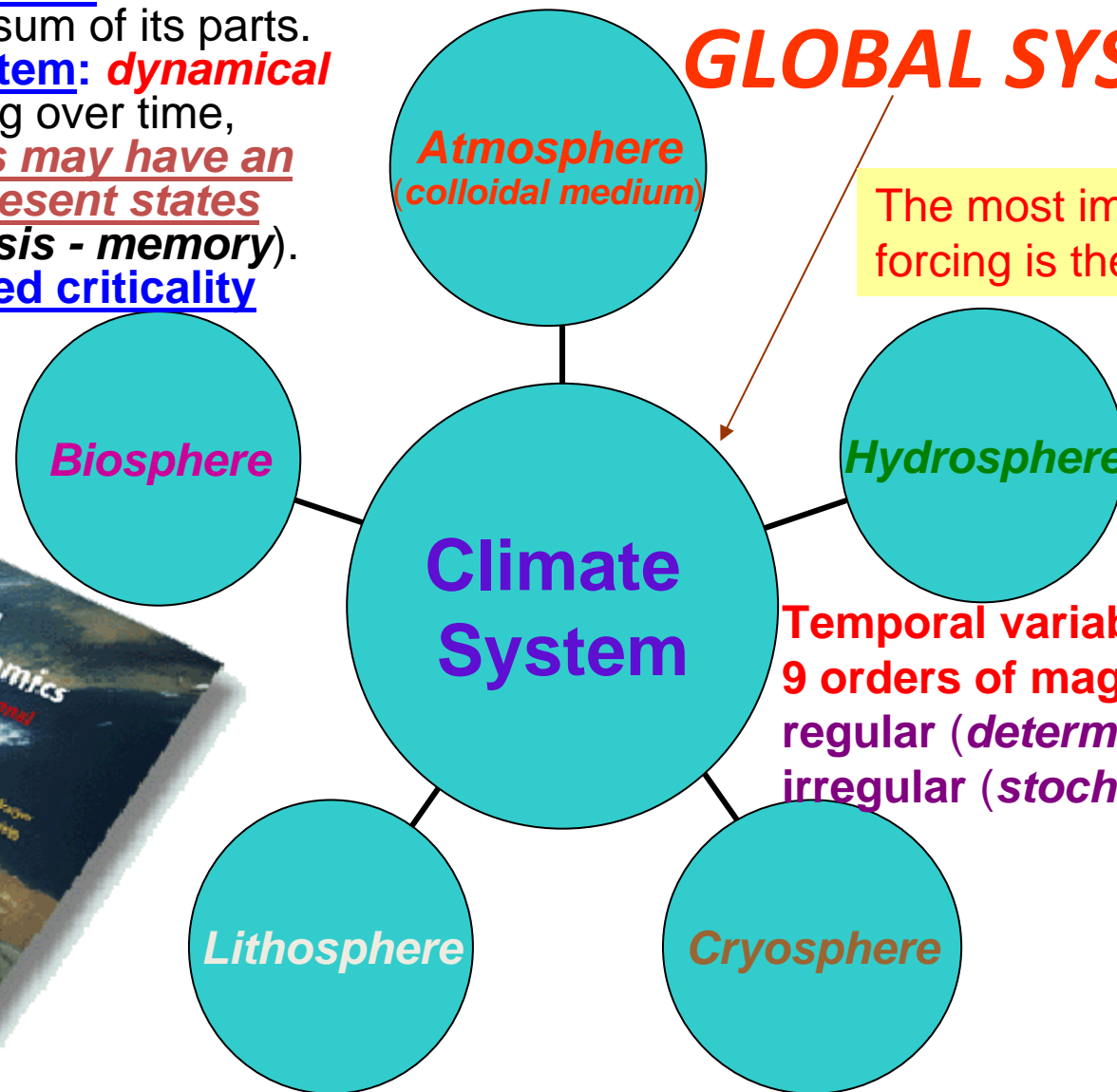
University of Athens, Greece

covar@phys.uoa.gr

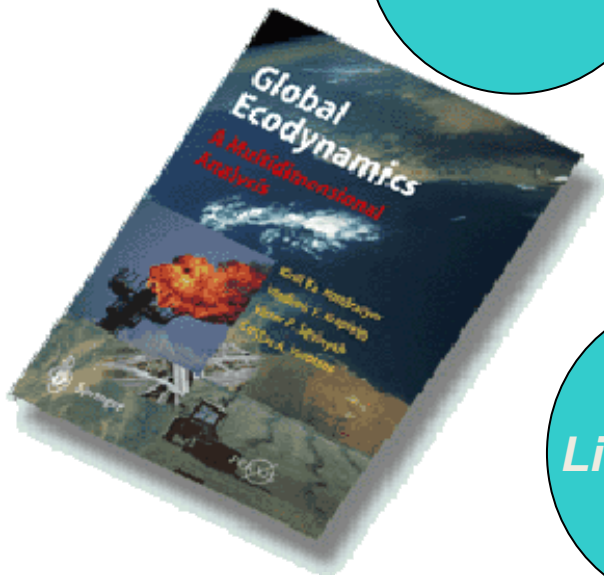
- 1) **nonlinear system**: it can't be expressed as a sum of its parts.
- 2) **complex system**: *dynamical system* changing over time, and *prior states may have an influence on present states* (exhibit *hysteresis - memory*).
- 3) **self-organized criticality**

GLOBAL SYSTEM

The most important external forcing is the **Sun**



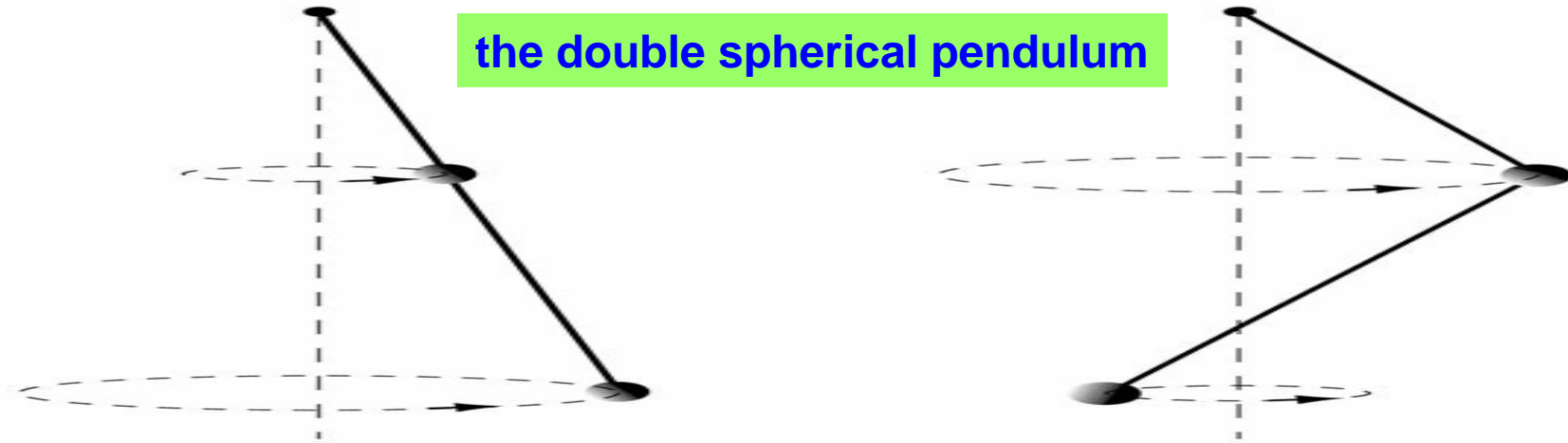
Temporal variability spans: **9 orders of magnitude** due to regular (*deterministic*) and irregular (*stochastic*) changes



K. Kondratyev, V. Krapivin, P. Savinykh, C. Varotsos, SPRINGER, 723 p, 2004.

Interaction 1: Radiative forcing: $\Delta T \propto \tau_c X S$: relax. time X clim. sens.

Interaction 2: Dissipation-induced instabilities



The straight-stretched-out branch is *stable*

The cowboy branch is *susceptible to dissipation-induced instabilities*

A famous example-*Sputniks* (a basketball) - *Explorer I* (long and narrow like a pencil)



Explorer I was supposed to rotate around its axis of minimum moment of inertia and not that of the maximum moment of inertia and *made just one Earth orbit.*

This instability was caused by a flexing of its antennae, which dissipated a small amount of rotational energy.





PART I:

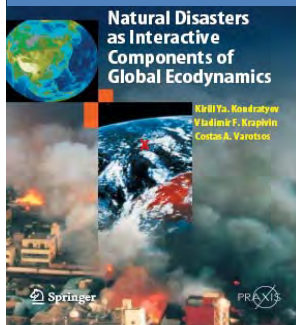
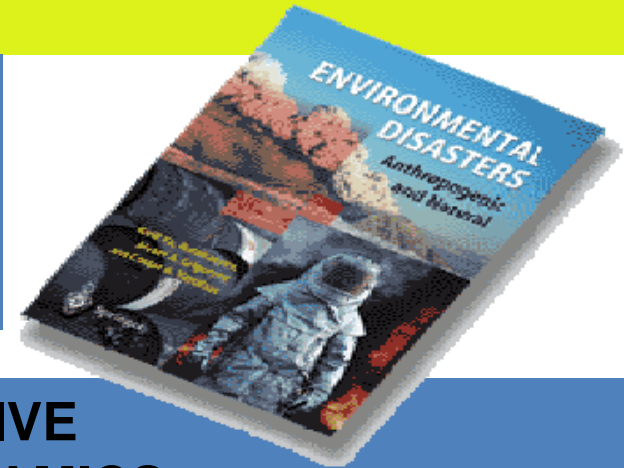
Detection of long-memory effects

**Long-range correlations in time-series
of basic global atmospheric parameters
(DFA: CO_2 , T , O_3)**

**(fluctuations in small boxes are related to those in larger boxes
in a power-law fashion)**

ENVIRONMENTAL DISASTERS: Anthropogenic and Natural

K. Kondratyev, A. A. Grigoryev, C. A. Varotsos,
SPRINGER -Praxis, 528 pages, 2002.



NATURAL DISASTERS AS INTERACTIVE COMPONENTS OF GLOBAL ECODYNAMICS

K. Ya. Kondratyev,, V. F. Krapivin, C. A. Varotsos,
SPRINGER – Praxis, 2006.

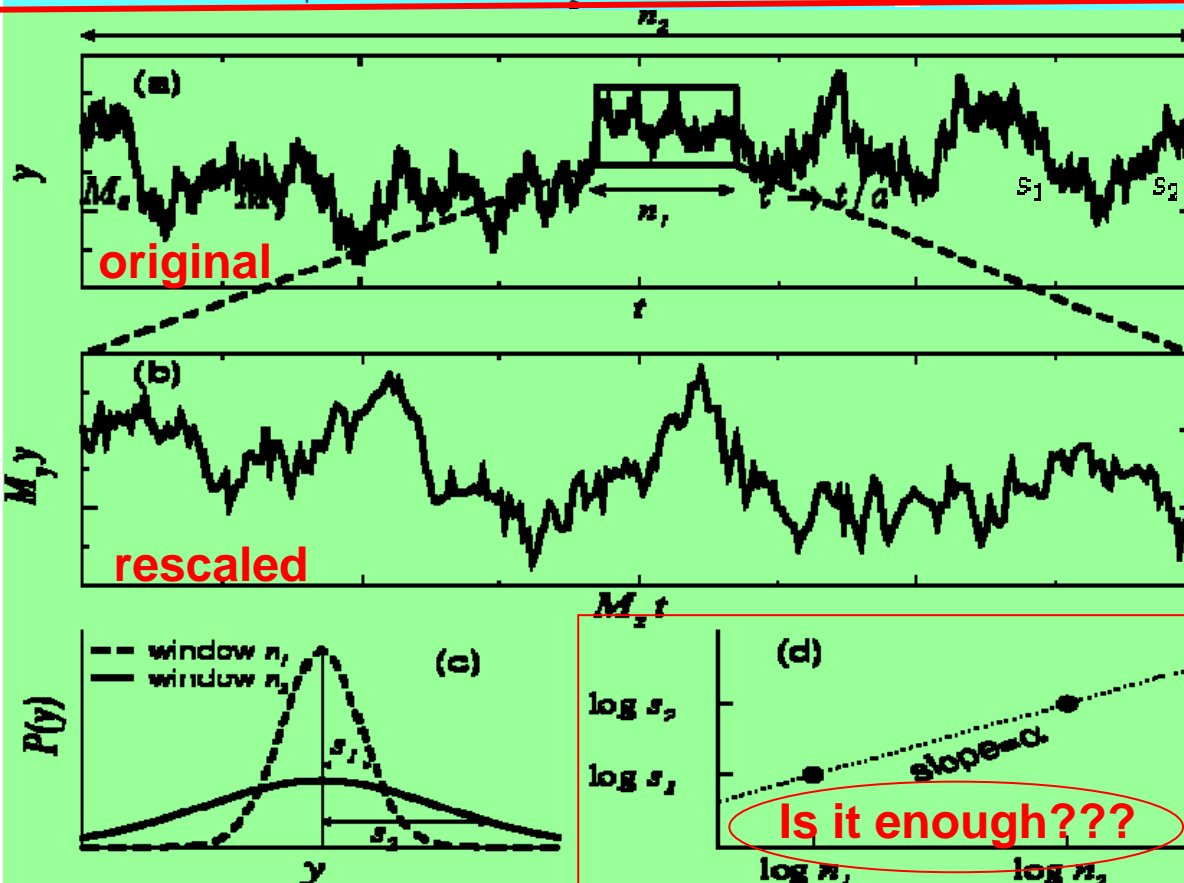
Self-similarity embedded in a time-series



$$f(x) = \sum_{n=0}^{\infty} a^n \cos(b^n \pi x),$$

$$0 < a < 1 \quad ab > 1 + \frac{3}{2}\pi.$$

prior states may have an influence on present states



$$y(t) \stackrel{d}{=} \alpha^x y\left(\frac{t}{a}\right)$$

with the proper choice of scaling factors M_x and M_y the rescaled time series resembles the original one

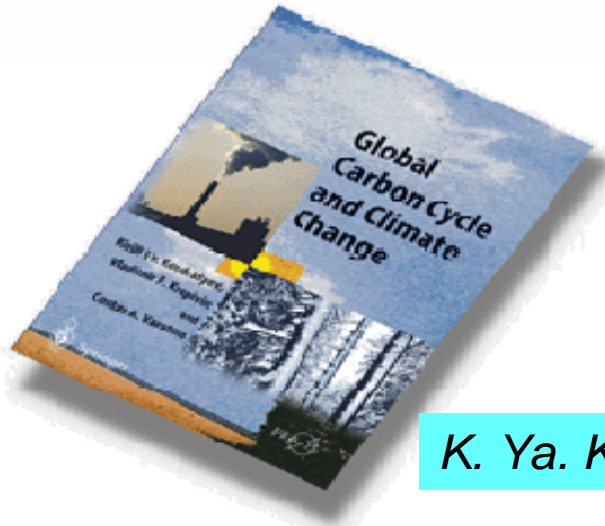
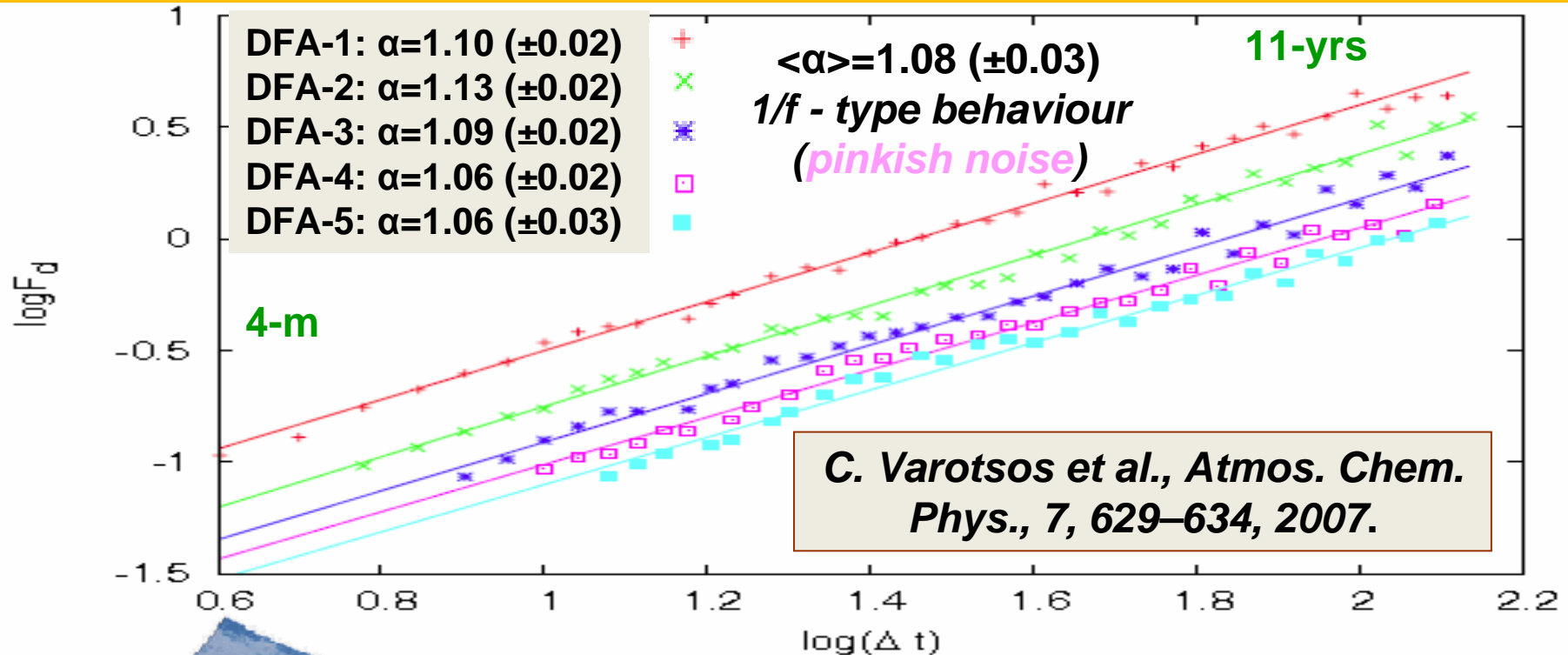
$$M_x = n_2/n_1 \quad M_y = s_2/s_1$$

$$\alpha = \frac{\ln M_y}{\ln M_x} = \frac{\ln s_2 - \ln s_1}{\ln n_2 - \ln n_1}$$

s_1, s_2 : st. dev. of y fluctuations, $P(y)$: probability distribution

Question: Is there any scaling in the temporal CO₂

fluctuations?
DFA on CO₂: 1) Mauna Loa Obs. (19.5°N, 155.5°W) 1959–2004

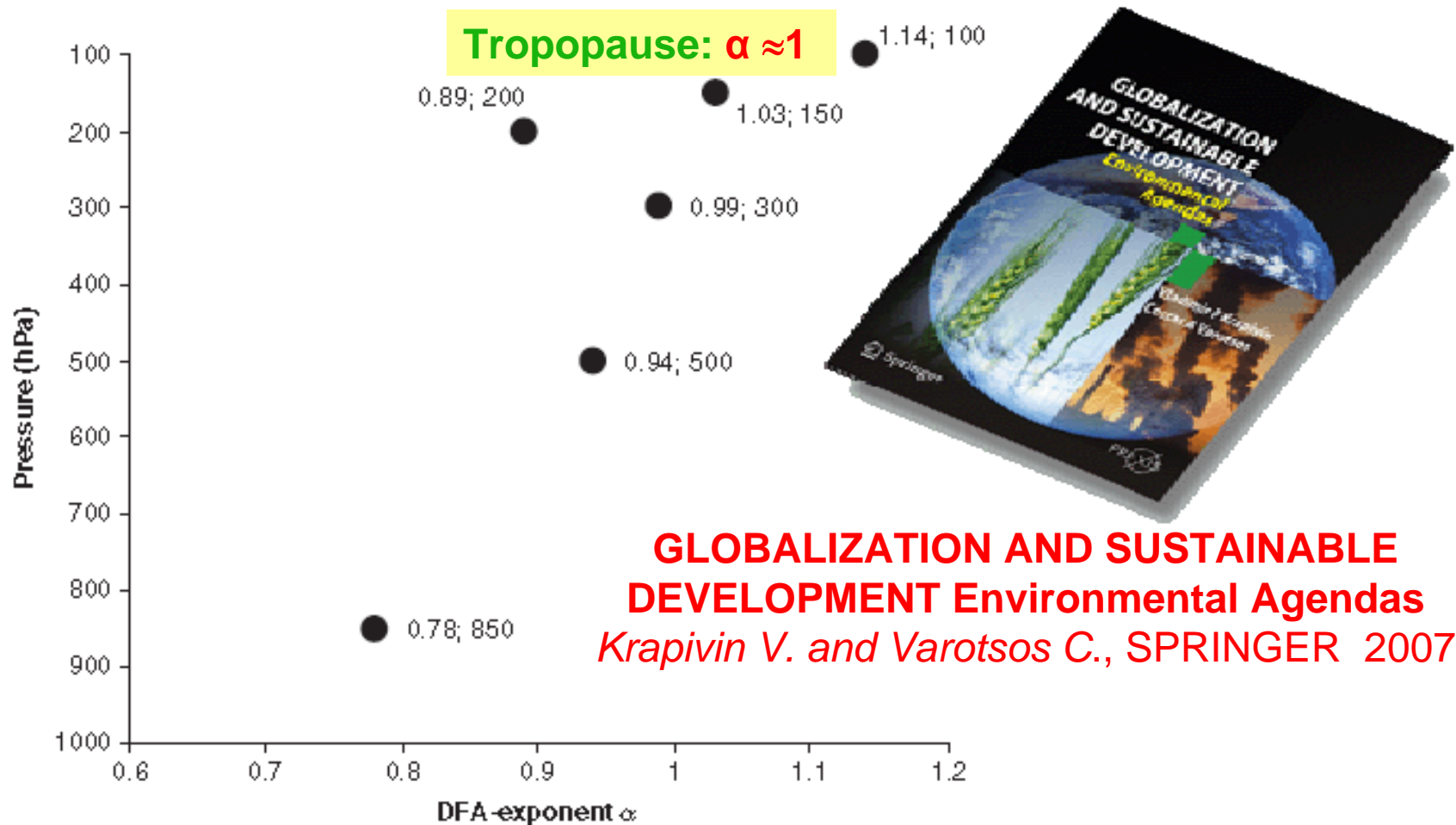


2) Antarctica (90°S, 24.7°W) CO₂ time series 1973–2004: $\langle \alpha \rangle = 1.12 (\pm 0.03)$

Result: The CO₂ fluctuation in the “following time interval” will be the same as in the corresponding “current time interval”.

K. Ya. Kondratyev, V. F. Krapivin, C. A. Varotsos, Springer, 2003

On the altitude dependence of the temperature scaling behaviour at the global troposphere (*Varotsos et al. IJRS, 31, 2010, 343–349*)

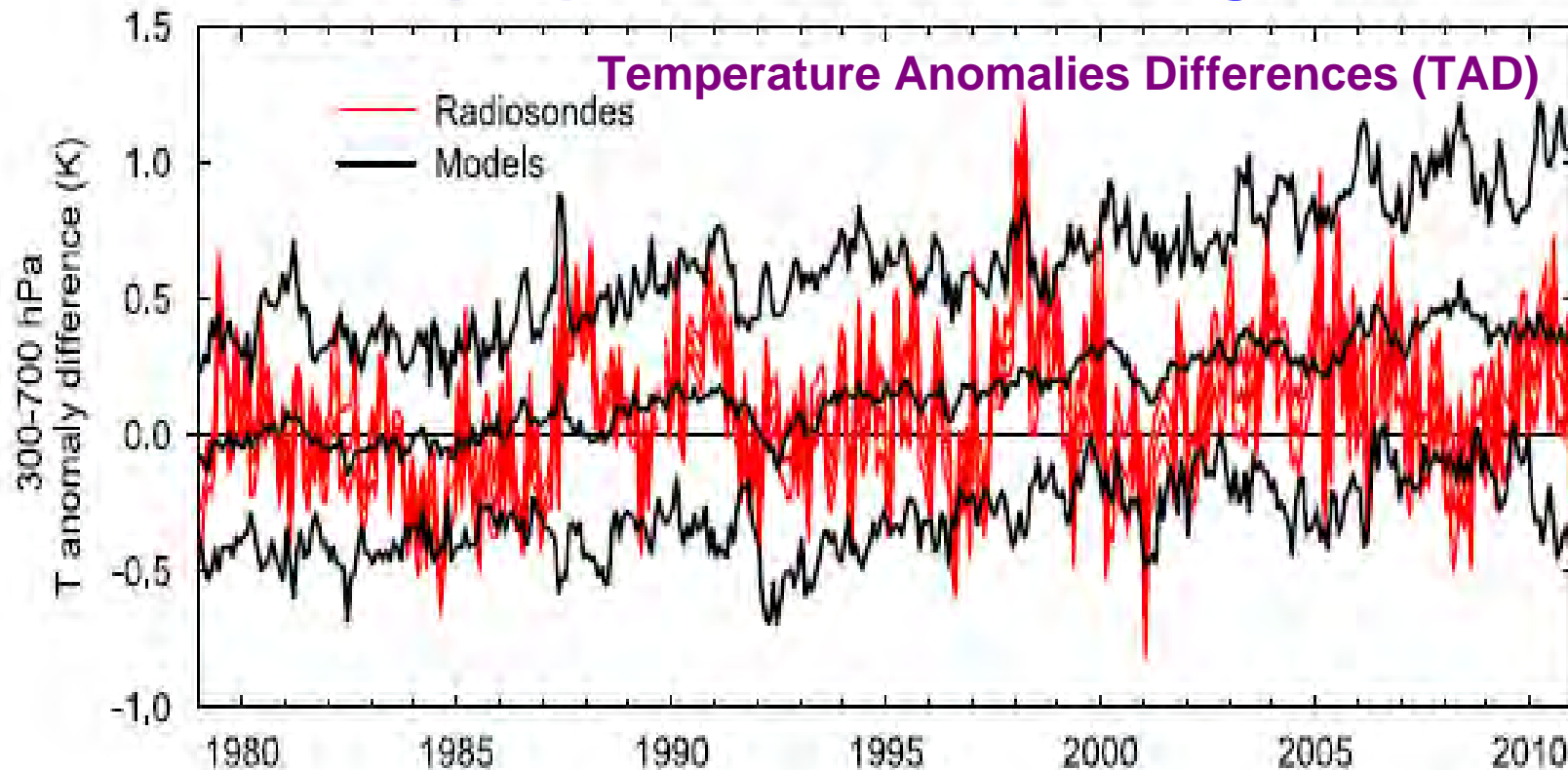


Result: There is long-range power-law persistence in the global tropospheric temperature fluctuations, which becomes stronger as the altitude increases.

Varotsos et al. 2009, Scaling behaviour of the global tropopause, ACP, 9 677-683

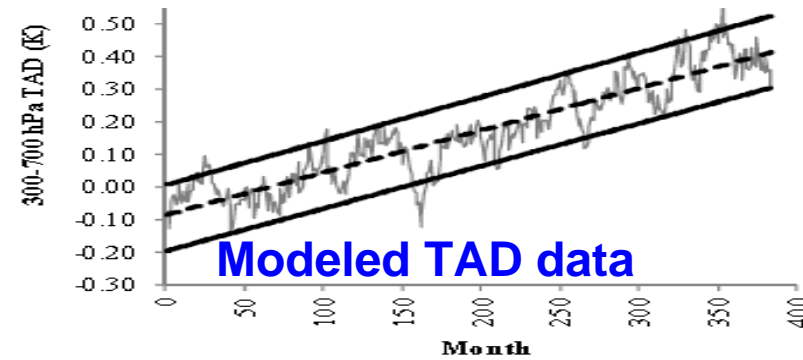
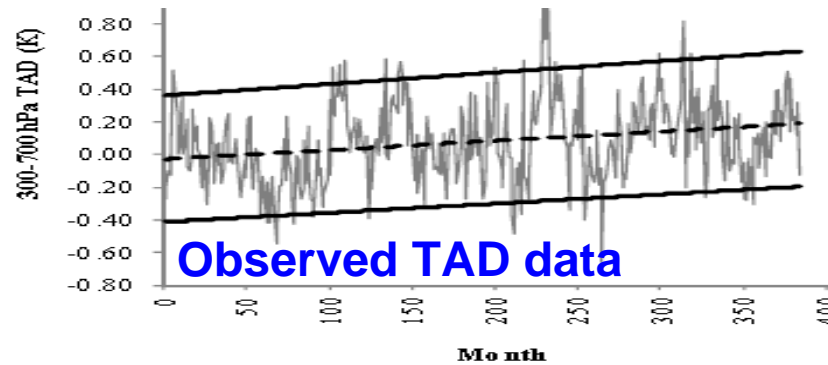
Reasons for the **inconsistencies** between the **modelled** and **observed** temperatures in the tropical troposphere
Varotsos et al., GRL, 2013 (in press)

Tropospheric vertical warming ???

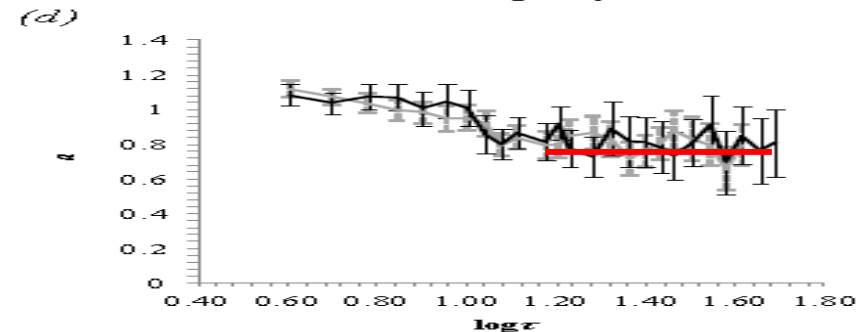
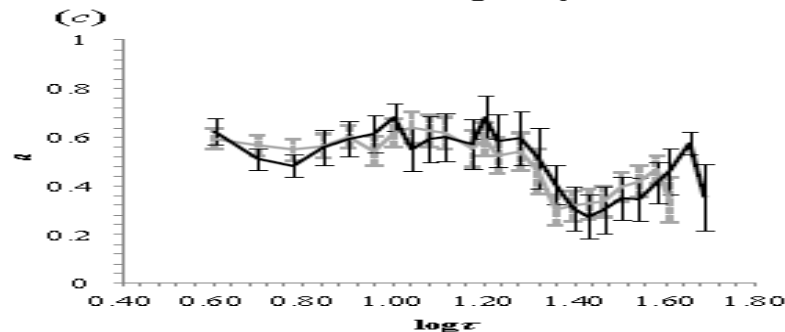
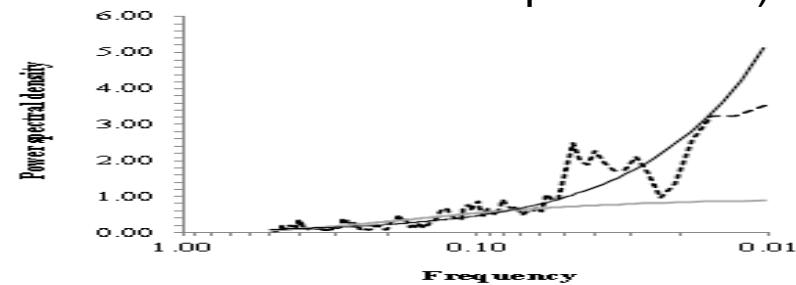
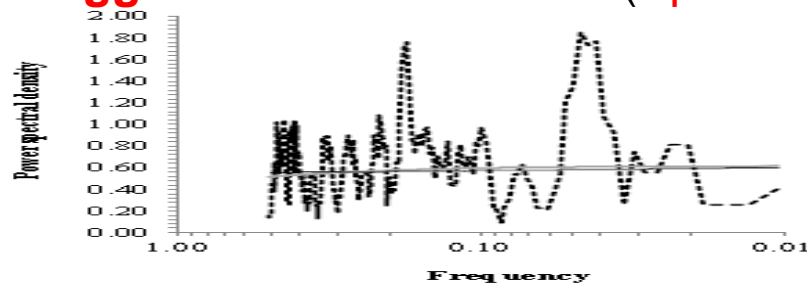


Monthly 300-minus-700 hPa tropical (20°N – 20°S) temperature anomalies (TAD) for 1979–2010, based on mean 2 standard deviations of **5 radio-sonde datasets** and **36 climate model simulations**.

The vertical amplification of warming by models



The trend of the modeled TAD data is significantly higher than that of the measured ones confirming that **the vertical amplification of warming is exaggerated in the models** (“quantile regression” on 5th and 95th percentiles).



Conclusion: The modelled TAD data suffer from a power-law signal. It must be taken into account in attempts to improve the modeled temperature data

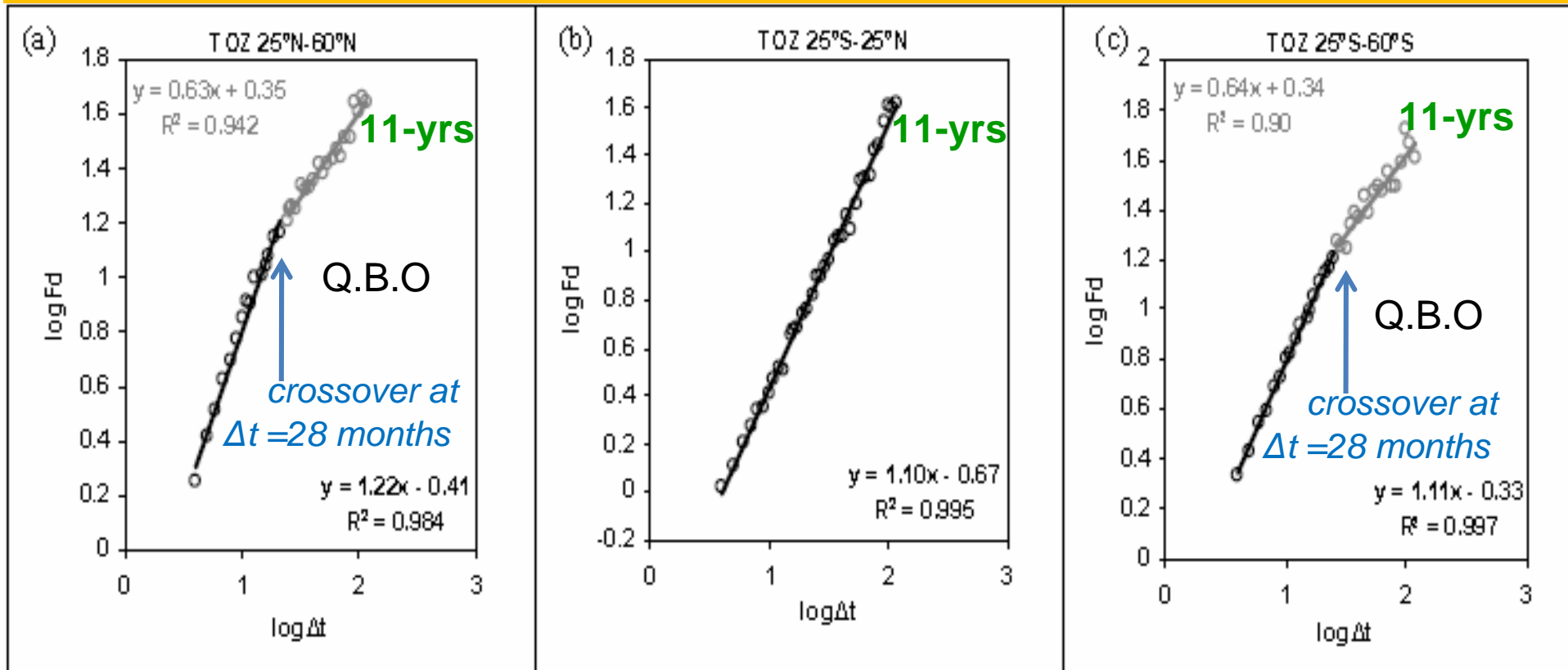
Observational evidence for chemical ozone depletion over the Arctic in winter 1991–92

P VON DER GATHEN, M REX, NRP HARRIS, D LUCIC, BM KNUDSEN, GO BRAATHEN, H DE BACKER, R FABIAN, H FAST, MGIL, E KYRÖ, I MIKKELSEN, M RUMMUKAINEN J STÄHELIN & C VAROTSOS

...The approaches used previously have often been indirect, typically relying on relationships between ozone and long-lived tracers. Most recently Manney et al. used such an approach, based on satellite measurements, to conclude that the observed ozone decrease of about 20% in the lower stratosphere in February and March 1993 was caused by chemical, rather than dynamical, processes. Here we report the results of a new approach to calculate chemical ozone destruction rates that allows us to compare ozone concentrations in specific air parcels at different times, thus avoiding the need to make assumptions about ozone / tracer ratios. For the Arctic vortex of the 1991-92 winter we find that, at 20 km altitude, chemical ozone loss occurred only between early January and mid February and that the loss is proportional to the exposure to sunlight. The timing and magnitude are broadly consistent with existing understanding of photochemical ozone-depletion processes.

Question: Long memory in **total ozone** ?

DFA on TOZ data of the WMO Dobson Network, 1964–2004



Log-log plot of the TOZ root-mean-square fluctuation function (F_d) versus temporal interval Δt (in months) over the tropics, and mid-latitudes of both hemispheres.

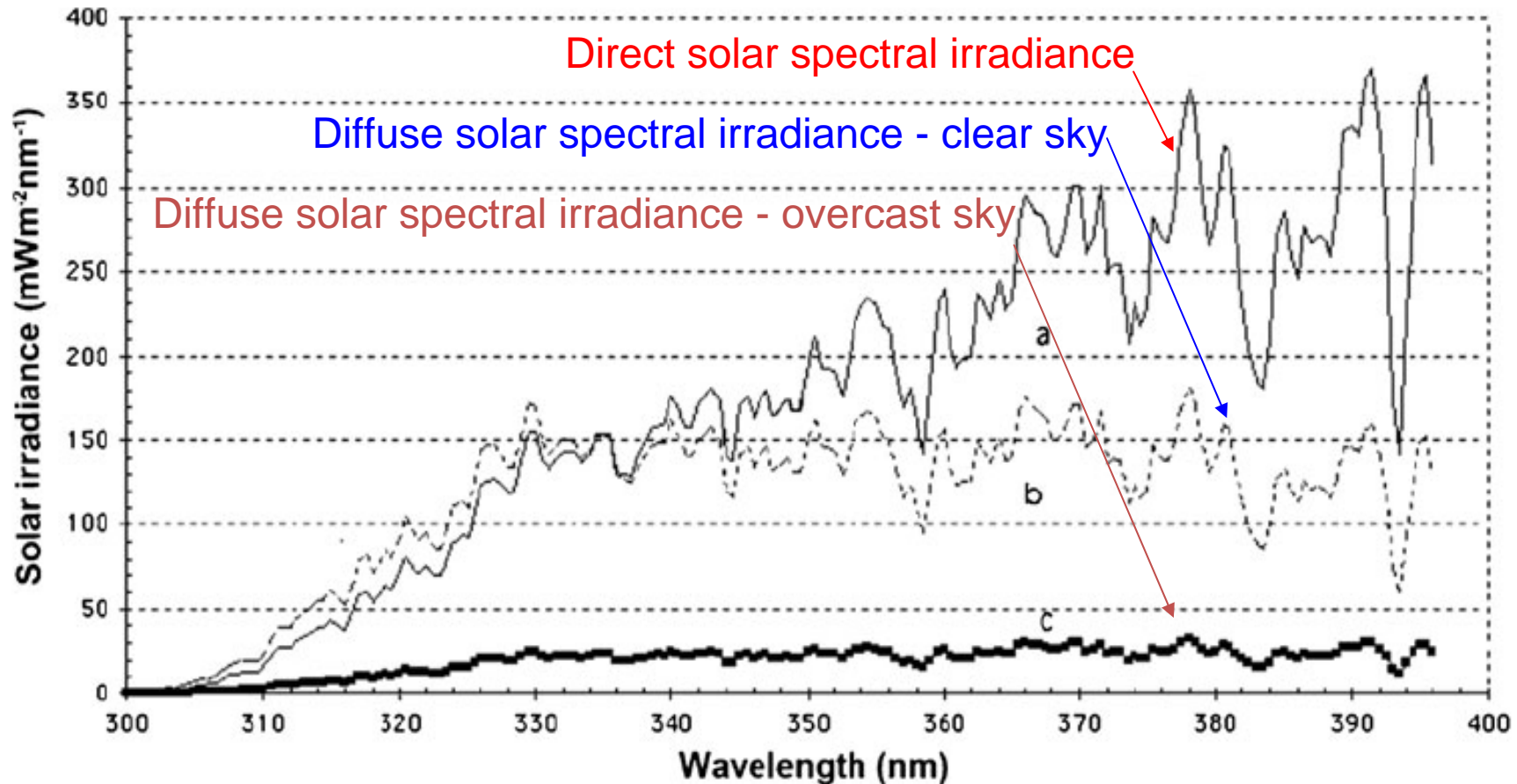
Result: The exponent at long time scales is larger in tropics ($\alpha \approx 1$) than in the mid-latitudes. Greater persistence in the tropics could be a result of either stronger positive feedbacks or larger inertia than in the mid-latitudes.



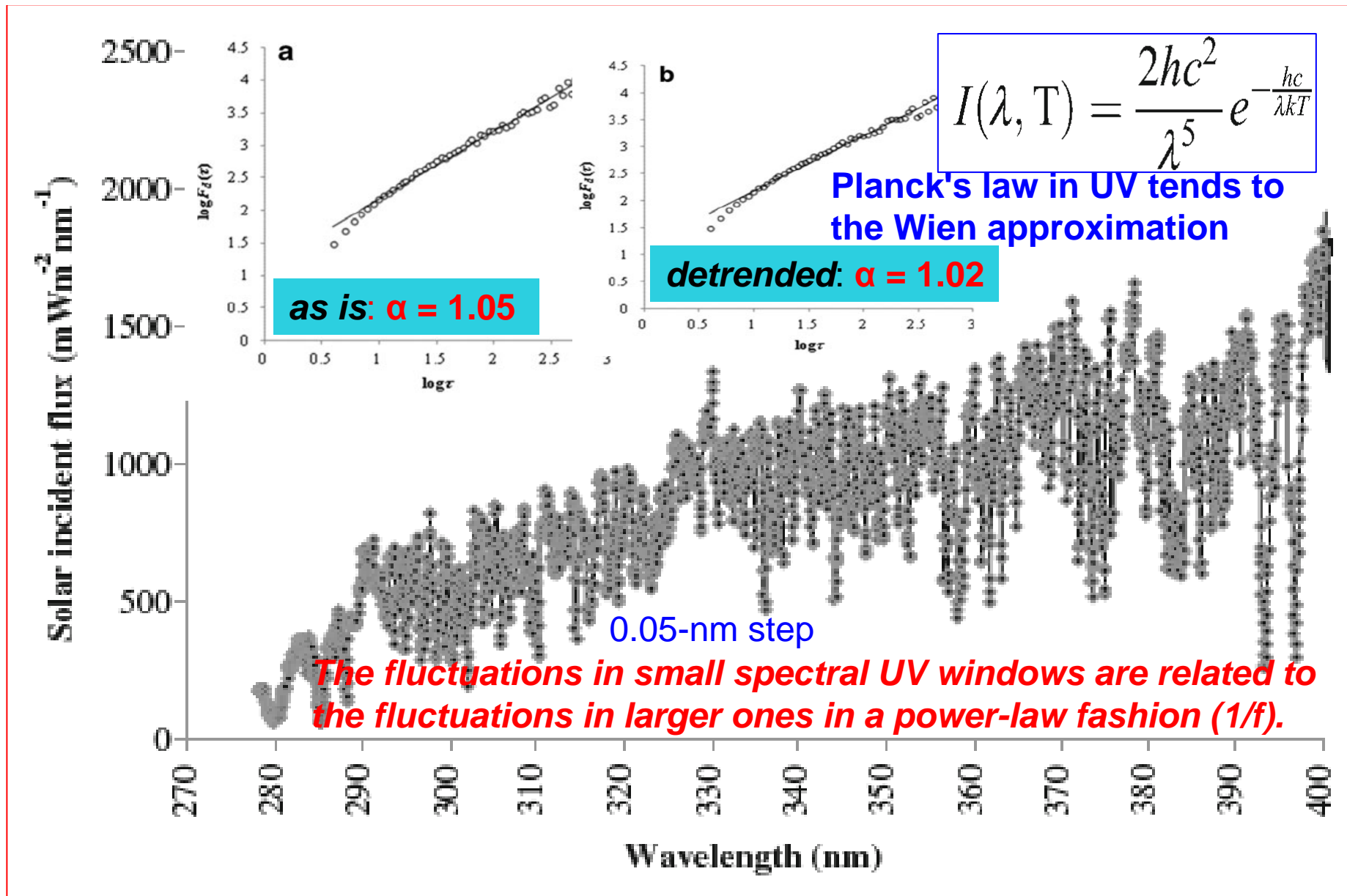
C Varotsos, D Kirk-Davidoff, 2006 Scaling in ozone and temperature, ACP, 6, 4093

1/f noise in the UV solar spectral irradiance

Varotsos et al., (2013) *Theor Appl Climatol* 111:641–648



a) Direct and **b)** diffuse solar irradiance spectra recorded on an horizontal plane at the ground on a clear sky day (17/9/2000) and **c)** diffuse solar irradiance spectrum recorded at the same site on an overcast sky day (20/9/00)

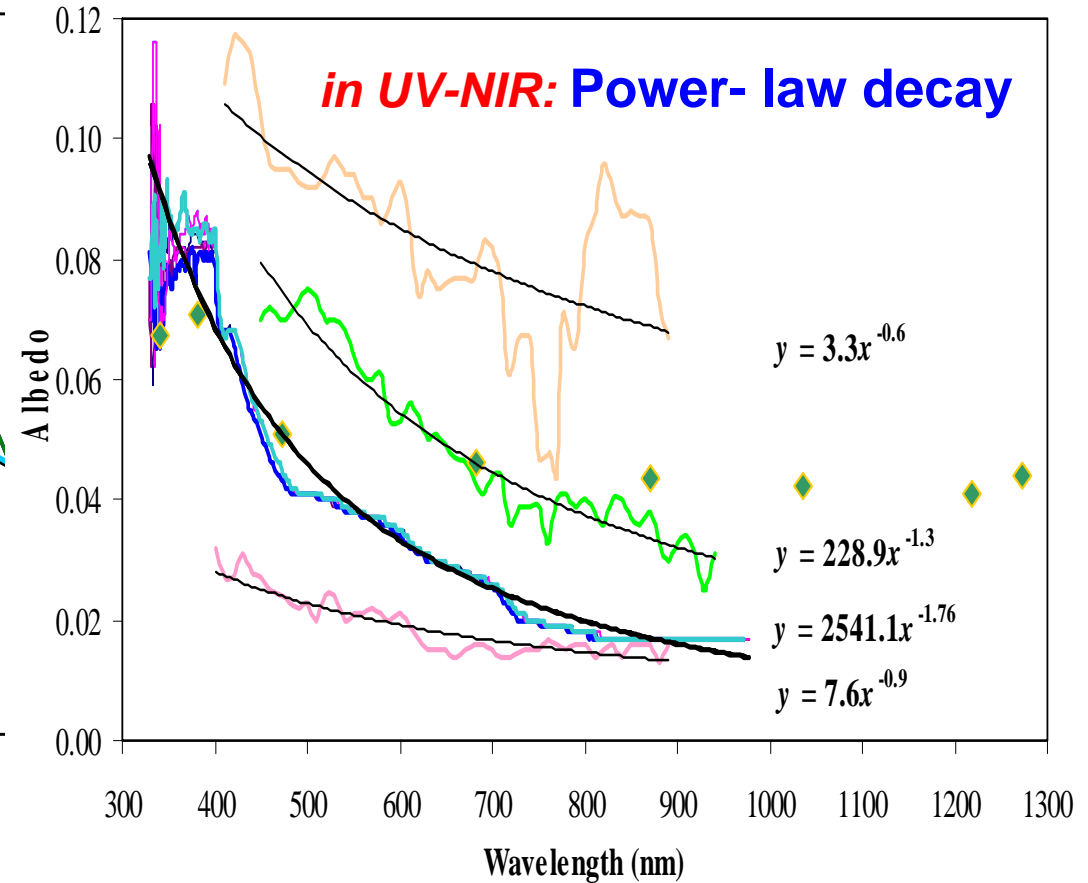
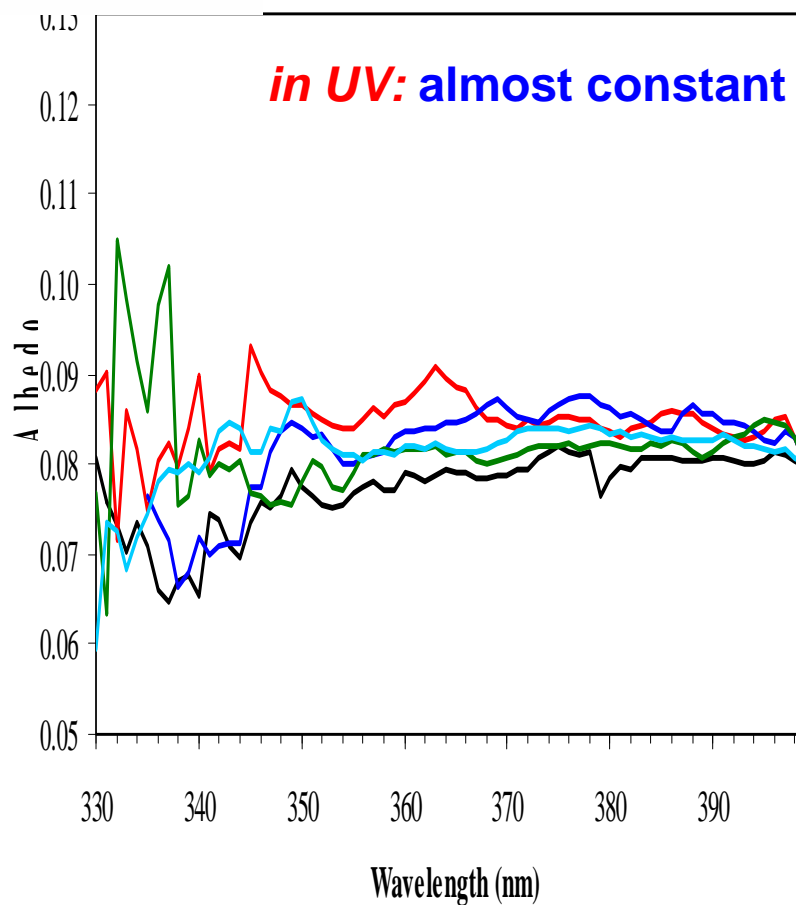


Varotsos et al., (2013) TAAC, 111: 641–648 and complementary note

Similar results were obtained at every ½ hr from nearly sunrise to sunset



PART II: Spectral dependence of albedo *a. The case of water in UV*

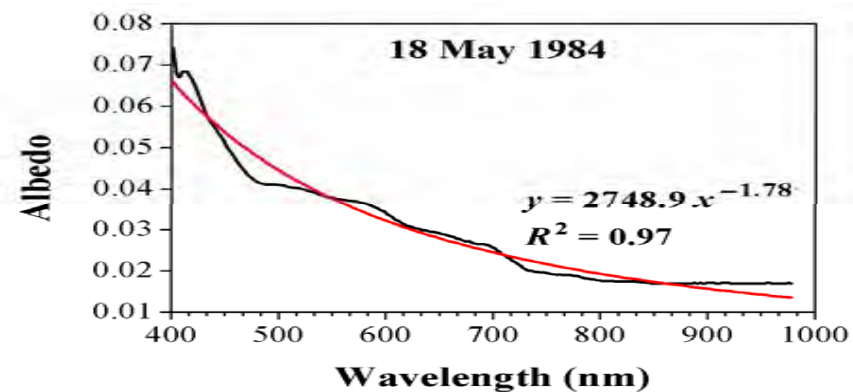
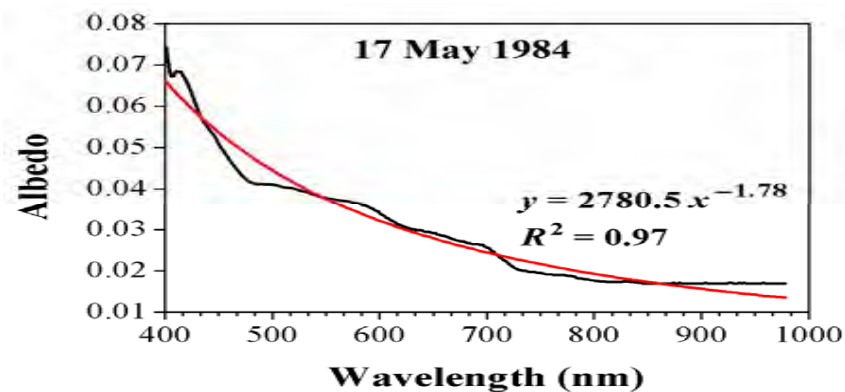
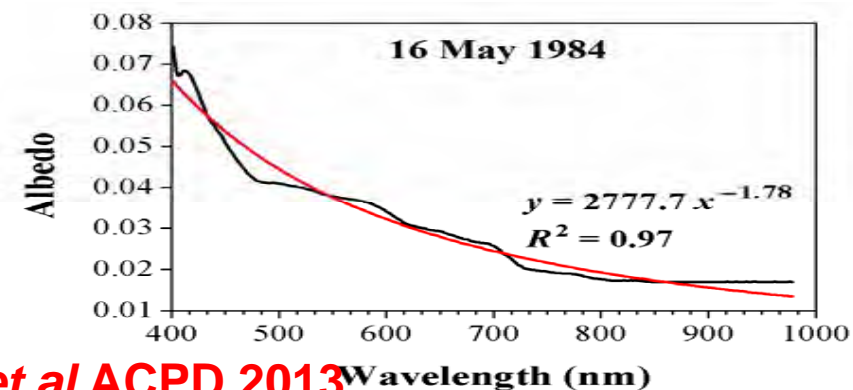
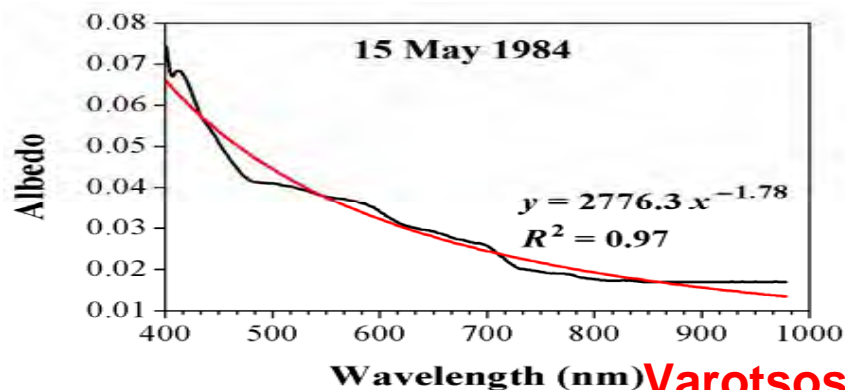
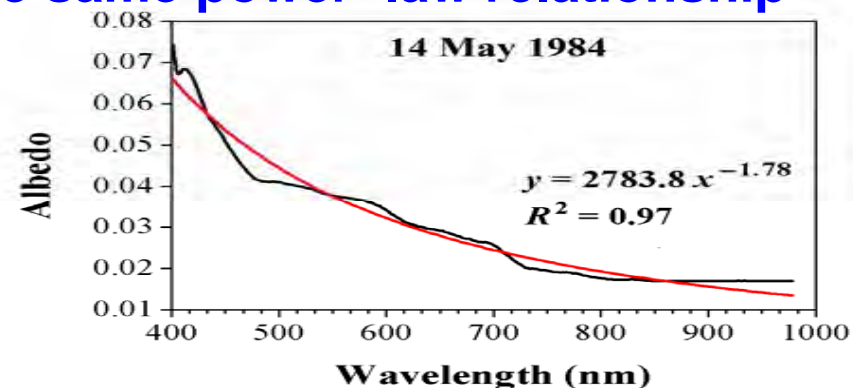
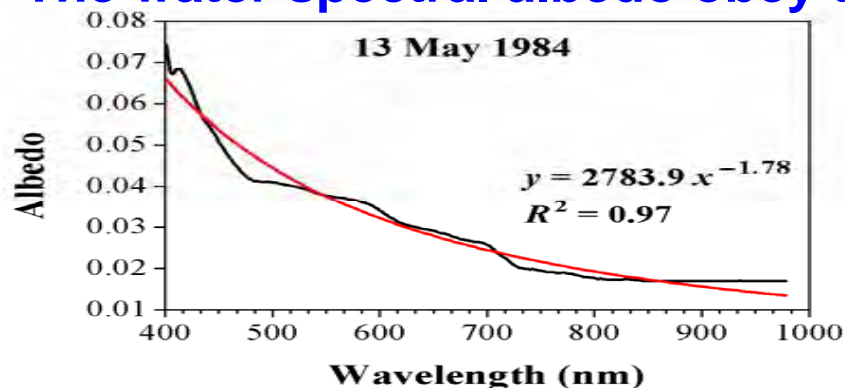


Varotsos, C. et al., 2013: *New spectral functions of the near-ground albedo derived from aircraft diffraction spectrometer observations*, Atmos. Chem. Phys. Discuss., 13, 16211-16245.

Spectral dependence of albedo

c. The case of water in visible-IR

The water spectral albedo obey the same power-law relationship



Varotsos et al ACPD 2013

Experimental findings about albedo

The near-ground albedo strongly depends on the wavelength spectrum and the ground surface, but **the current belief that the spectral albedo generally increases with increasing wavelengths for all kinds of surfaces is not valid** (e.g. see the case of snow).

- α. In the case of **water** surfaces the **albedo** in the **UV** is governed by rather **low wavelength dependence**. In the **visible and NIR** spectra **the water albedo obeys a constant power-law relationship** with wavelength.
- b. In the case of **sand** surface, the sand **albedo is a quadratic function of wavelength**, which becomes more accurate, if the UV is neglected.
- c. The spectral dependence of **snow** albedo behaves **similarly** to that of **water**, i.e. **both decrease from the UV to the NIR by 20-50%**, despite the fact that their values differ by one order of magnitude (water albedo being lower). The **snow** albedo versus **UV** wavelength is **almost constant**, while in the **visible-NIR** spectrum the best fit is achieved by a **second-degree polynomial**, with **opposite slope** to that of **sand**.

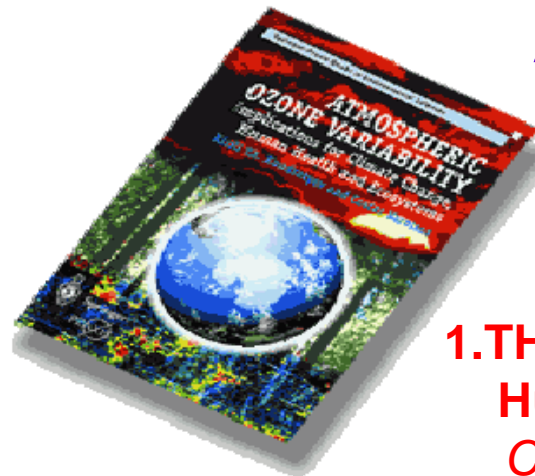
Varotsos, C. et al., 2013: Atmos. Chem. Phys. Disc., 13, 16211-16245.



PART III: *Predicting impending major events in climate dynamics*

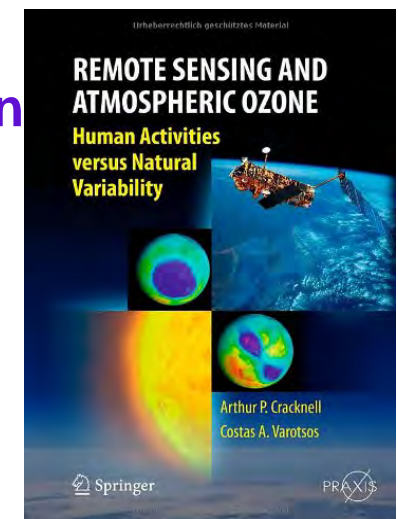
A case-study: the dynamical evolution of the ozone hole area over Antarctica

Varotsos et al., Atmos. Env. 2012, 47 , pp. 428-434



ATMOSPHERIC OZONE VARIABILITY:
Implications for Climate Change, Human
Health and Ecosystems *K. Kondratyev,*
C. Varotsos, SPRINGER, 624 p, 2000.

1.THE SCIENCE OF GLOBAL OZONE CHANGE:
Human activities versus natural variability,
Cracknell A., Varotsos C., SPRINGER, 2011.



Varotsos, *ESPR* 2002, 9, 375-376

This is the first journal paper stressing that the SSW over Antarctica in Sept 2002 was major leading to the ozone hole split. Until then it was believed that a major SSW was not feasible.

Abstract...

During September 2002, the ozone hole over the Antarctic was much smaller than in the previous six years. It has split into two separate holes, due to the appearance of sudden stratospheric warming that has never been observed before in the southern hemisphere. The analysis of this unprecedented event is attempted, regarding both the meteorological and photochemical aspects, in terms of the unusual thermal field patterns and the induced polar vortex disturbances.

Letters to the Editor

The Southern Hemisphere Ozone Hole Split in 2002

Costas Varotsos

University of Athens, Department of Applied Physics, Panepistimiopolis, GR-157 04 Athens, Greece
(covar@phys.uoa.gr, kvarots@cc.uoa.gr)

Among the most important aspects of the atmospheric pollution problem are the anthropogenic impacts on the stratospheric ozone layer, the related trends of the total ozone content drop and the solar ultraviolet radiation enhancement at the Earth's surface level.

During September 2002, the ozone hole over the Antarctic was much smaller than in the previous six years. It has split into two separate holes, due to the appearance of sudden stratospheric warming that has never been observed before in the southern hemisphere. The analysis of this unprecedented event is attempted, regarding both the meteorological and photochemical aspects, in terms of the unusual thermal field patterns and the induced polar vortex disturbances.

Introduction. The total ozone content (TOC) observations – currently performed by the Total Ozone Mapping Spectrometer (TOMS) flown on the NASA Earth Probe satellite and the NOAA-16 Solar Backscatter Ultraviolet instrument (SBUV/2) – showed that the size of the Antarctic ozone hole was around 15 million km² during the last two weeks of September 2002, which is well below the more-than 24 million km² seen during the last six years in this season. Apart from the smaller size (as it was in 1988), the Antarctic ozone hole split into two holes during late September, an event seen for the first time since global maps for the stratosphere of the southern hemisphere became available (Kondratyev and Varotsos 2000). According to the September 30 Press Release from NASA and NOAA (NASA/NOAA 2002), this year's warmer-than-normal temperatures around the edge of the polar vortex over Antarctica are responsible for the smaller ozone loss (Varotsos 2002) [Fig. 1].

This note attempts a better insight into this exceptional event through an analysis of the thermal field patterns over the Antarctic in late September; it proposes a plausible mechanism of this appearance.

Results and Discussion. According to the analysis of the climatological data, the coldest temperatures over Antarctica typically occur in August–September (depletion of the ozone layer), while temperatures usually begin to warm by early October (the ozone layer starts to recover). However, the corresponding data analysis shows that in late September 2002 (especially during 21–26/09/2002) some unusual synoptic features have occurred regarding the stratospheric weather patterns over Antarctica. In particular, an inspection of the polar stereographic charts (10 hPa geopotential height) shows that the basic polar vortex in the stratosphere of the southern hemisphere was step-by-step elongated up to the occurrence of a dramatic change – the polar vortex split into two centres. To be more concrete, on September 21 the basic polar vortex elongated (as shown by the roughly elliptical height contours) and centered just off the pole. On September 22, this structure rotated eastward and elongated further with a weakening of the polar vortex (accompanied by a quasi-stationary anticyclone which appeared much earlier than normal) at the middle. On September 23 and 24 this rotation and elongation continued, and the weakening became gradually stronger. On September 25, an opposite to the first, secondary anticyclone started to develop, and

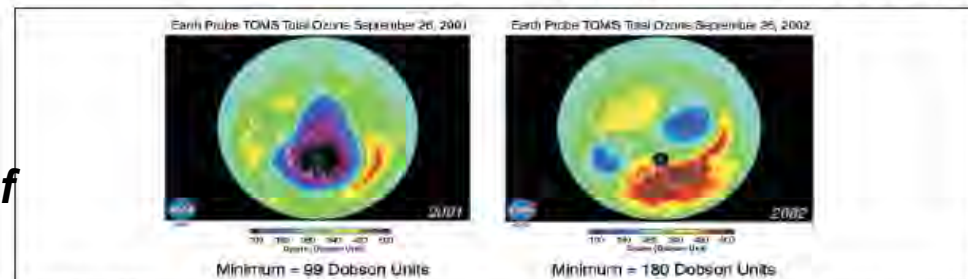
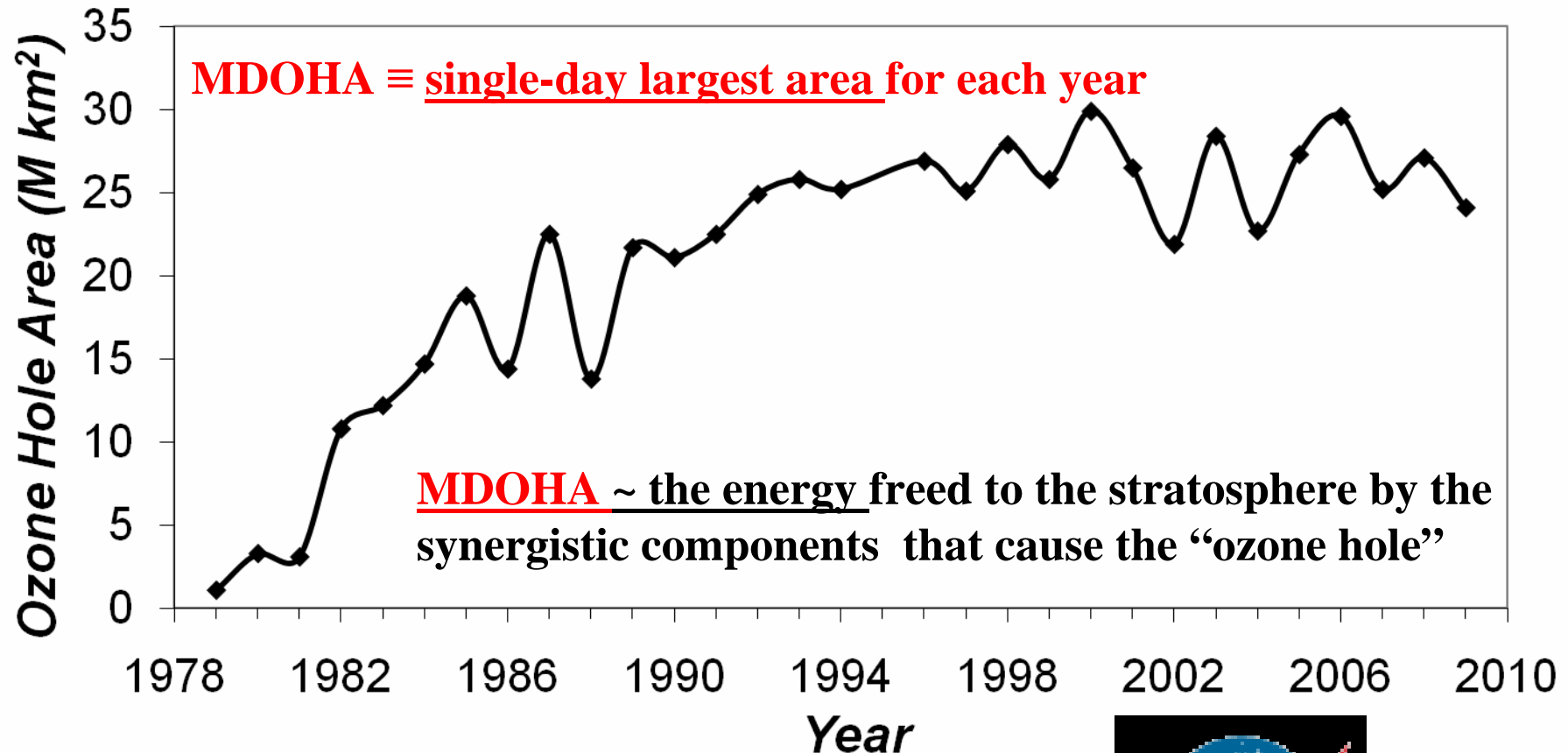


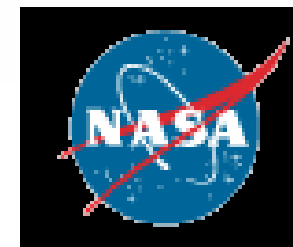
Fig. 1: What a difference a year makes. Southern hemisphere ozone image September 26, 2001 and 2002 (Source: http://toms.gsfc.nasa.gov/news/press_release_2002.html)

2. Data

The maximum daily ozone hole area (MDOHA) for each year vs. the date of occurrence over Antarctica for the 1979-2009 period.



Data source: Ozone Hole Watch



3. A new tool

Method “Natural Time Analysis” (NTA)

which enables the identification of the time of the extreme event occurrence (within a time window before it occurs).

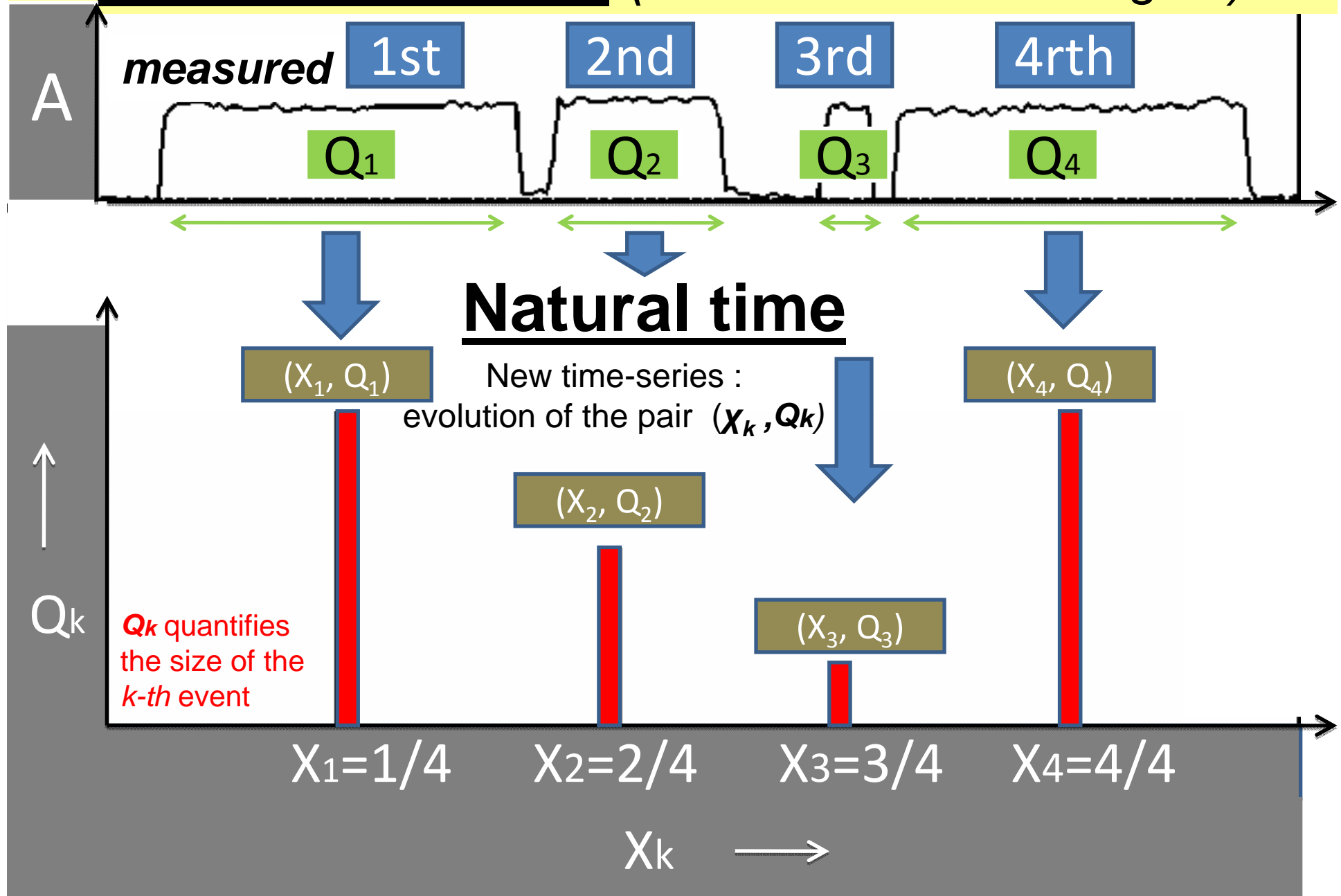
STEP 1. Conversion of the original time series to a new one disregarding the temporal sequence of the event occurrence

In the original time series (MDOHA) comprising N events,

$$\text{the natural time } (X_k) \equiv \frac{\text{Order of occurrence of an event } (k)}{\text{Total number of the events } (N)}$$

X_k (with values between **zero and unity**) serves as an index for the occurrence of the k -th event.

Conventional time (case: dichotomous signal)



STEP 2. Calculation of the entropy (S)

We calculate the “probability” to observe the transient at natural time χ_k : $p_k = Q_k / \sum_{n=1}^N Q_n$, then:

$$\langle \chi \rangle = \sum_{k=1}^N p_k \chi_k \quad \text{and} \quad \langle \chi \ln \chi \rangle = \sum_{k=1}^N p_k \chi_k \ln \chi_k$$

Then, **the entropy S (dynamic entropy)**, defined as:

$$S \equiv \langle \chi \ln \chi \rangle - \langle \chi \rangle \ln \langle \chi \rangle \quad \text{becomes:}$$

$$S \equiv \sum_{k=1}^N p_k \chi_k \ln \chi_k - \left(\sum_{k=1}^N p_k \chi_k \right) \ln \left(\sum_{m=1}^N p_m \chi_m \right)$$

A window of length (i) is sliding, each time by one year, through the whole time series. The entropy (S) is calculated each time.

Example: window of length $i=3$ events (years)

The maximum daily ozone hole area (MDOHA) value of the year 2000 will be involved in the calculation of (S) of the following 3-year sequences:

(1998, 1999, 2000), (1999, 2000, 2001), (2000, 2001, 2002).

corresponding to

$S_3(2000)$,

$S_3(2001)$,

$S_3(2002)$.

In other words, the (S) value will be calculated for each of these sequences after analyzing them in natural time, thus allowing the study of the evolution of S_3 step-by-

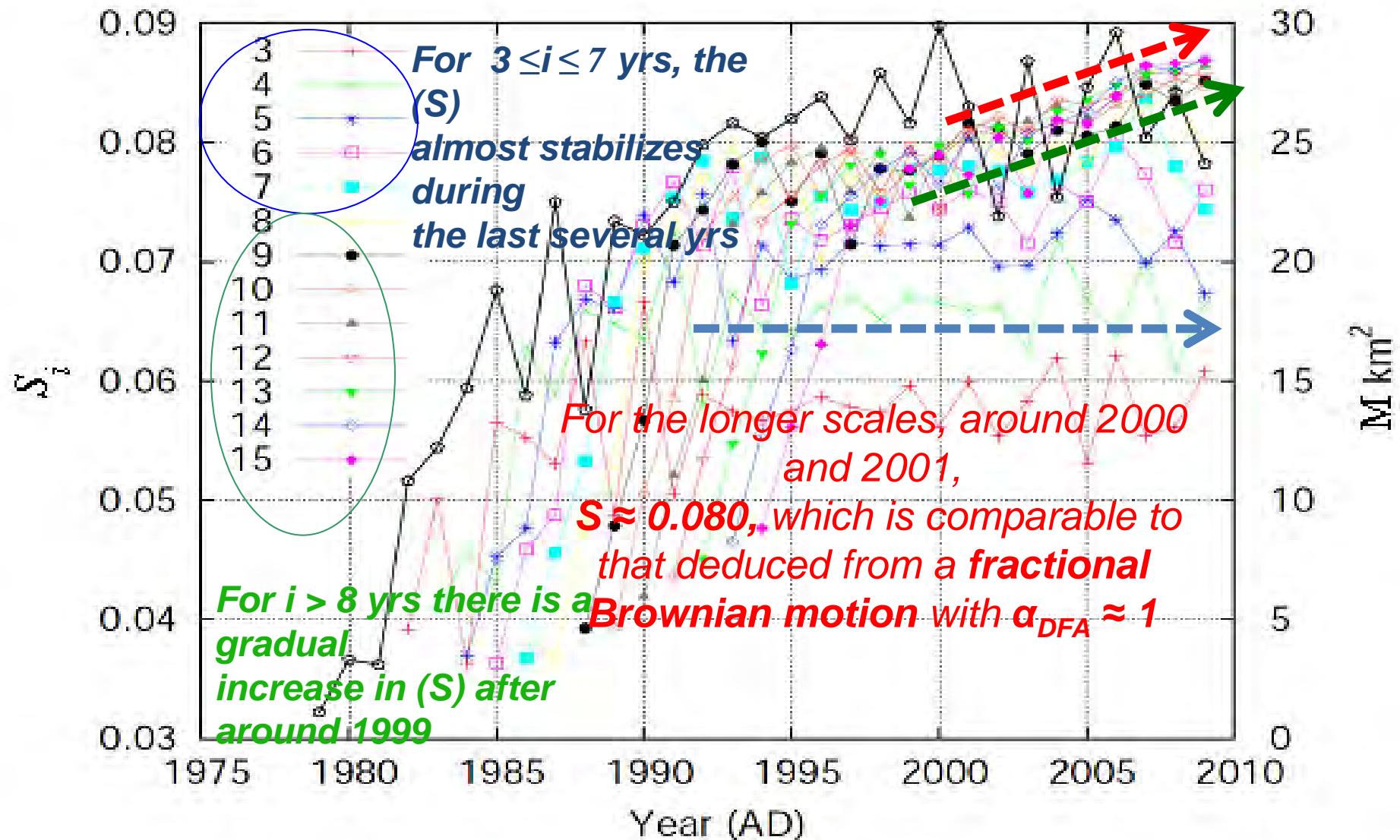


Fig. 1. The entropy S_i for window lengths $i = 3 \leq i \leq 7$ yrs (left scale) sliding each time by one year through the whole time series (1979-2009). The data (right scale) are

For critical dynamics $S < S_u (= \ln 2 / 2 - 1/4 \approx 0.0966)$ of a “uniform” distribution and exhibits long range correlations.

€

STEP 3. Calculation of the entropy (S_-) upon considering the time reversal

We calculate **the entropy** S_- upon considering **the time reversal** i.e., the operator \mathcal{T} , is defined by:

$\mathcal{T}P_k = P_{N-k+1}$ meaning that the **last event is now read as the first one**, the **last but one event as the second one**, etc.

“Uniform” distribution: $S = S_- = S_u (= \ln 2/2 - 1/4 \approx 0.0966)$

For critical dynamics: $S, S_- < S_u$

A window of length (i) is sliding, each time by one year, through the whole time series. The entropy S_- is calculated each time.

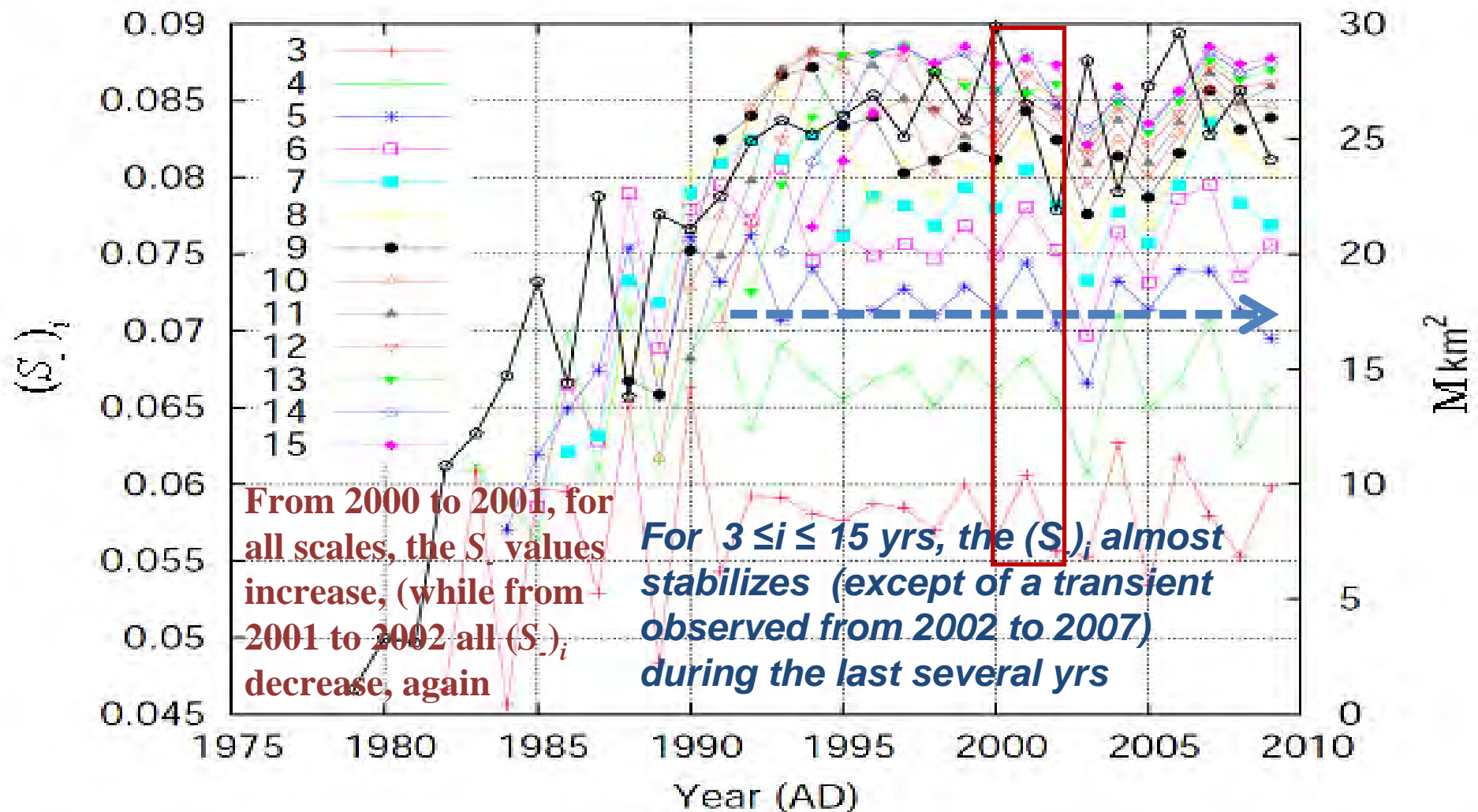


Fig. 2. The entropy in natural time under time reversal $(S_i)_i$ for window lengths $i = 3$ to 15 years (left scale) sliding each time by one year through the whole time series from 1979 to 2009. The experimental data (right scale) are depicted by

$(S_i)_i$ values remain smaller than that (S_u) of a “uniform” distribution.

STEP 4. Calculation of the difference (ΔS)

S: Past \rightarrow Future, S_- : Future \rightarrow Past, When coincidence occurs?

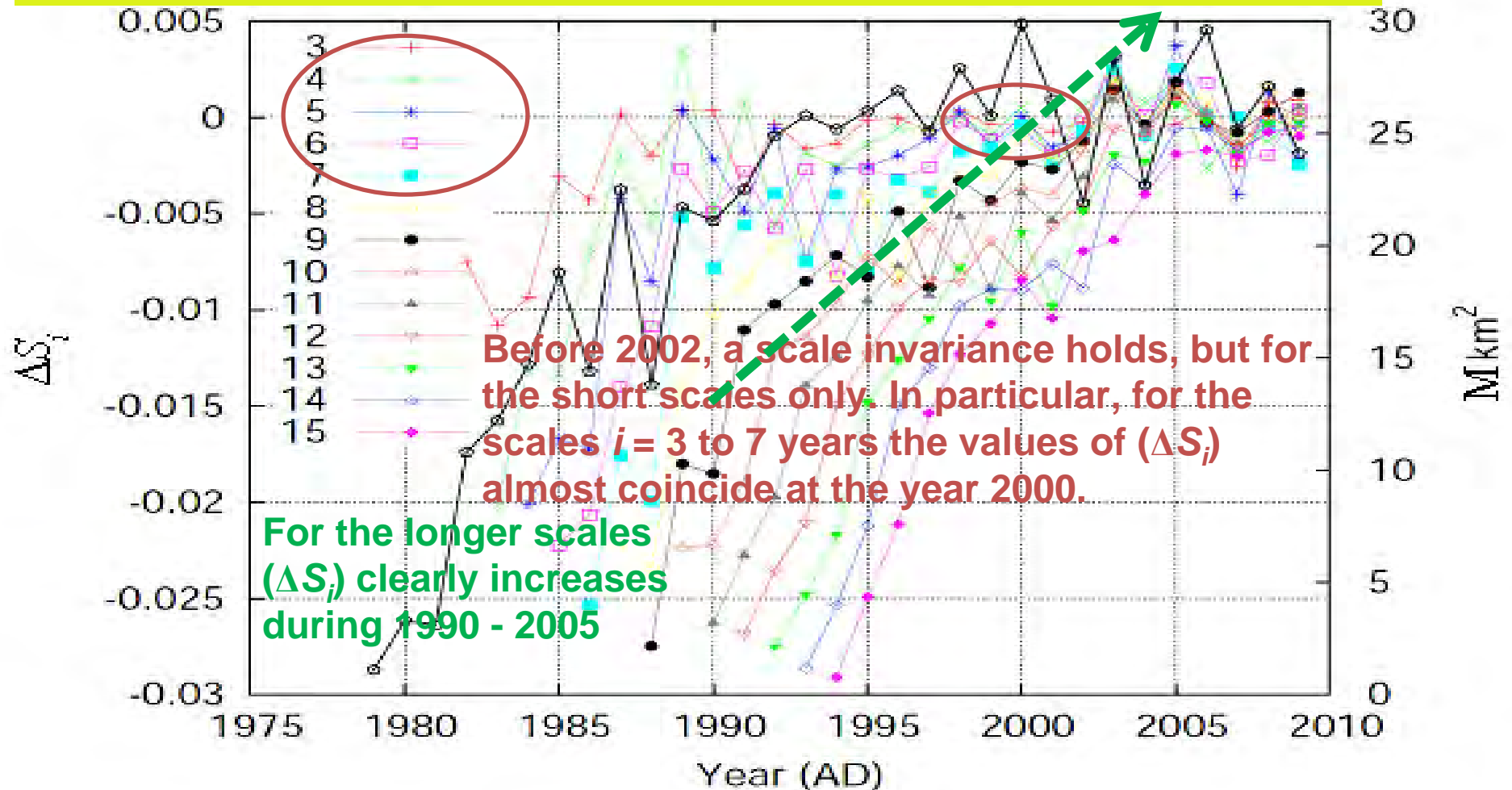
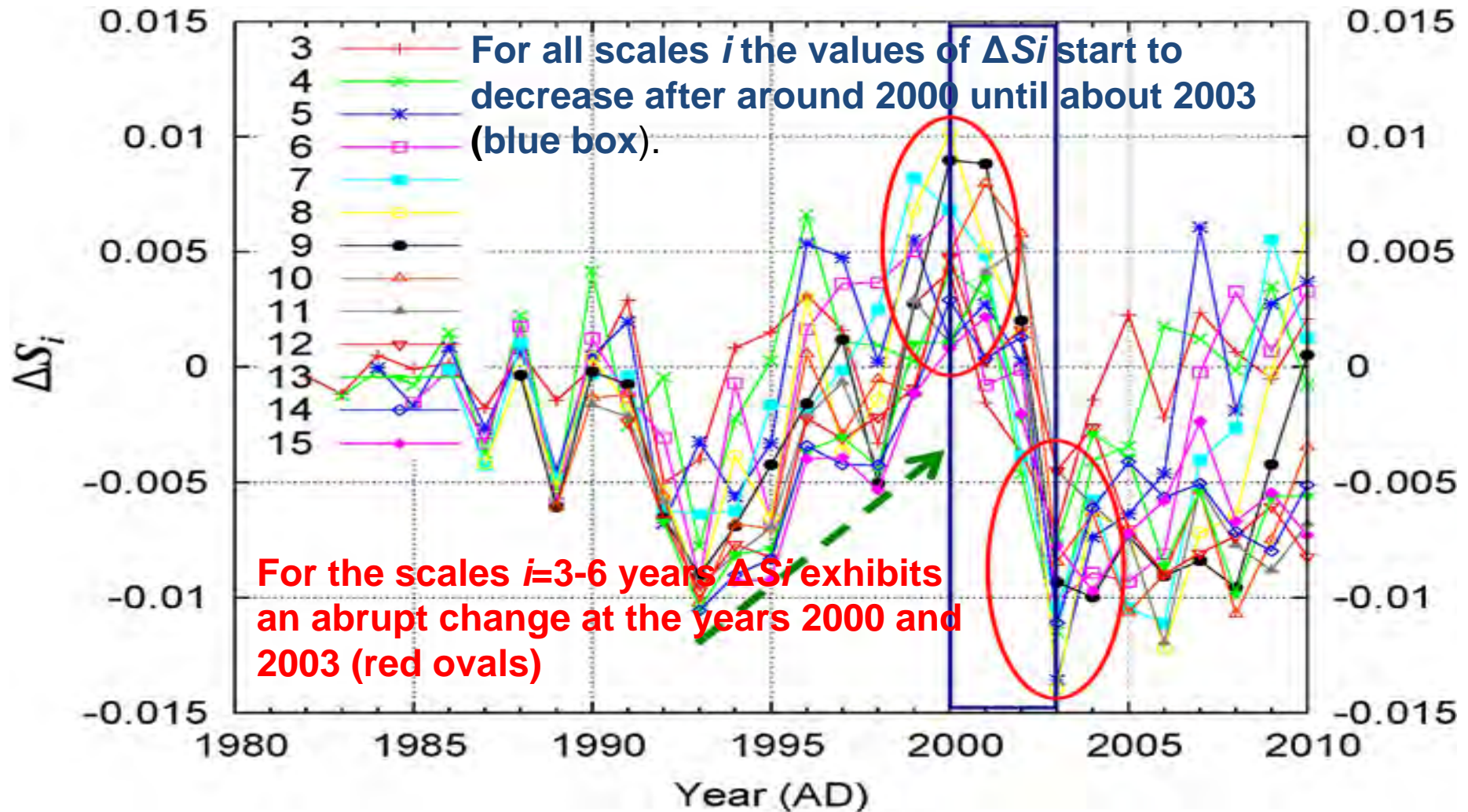


Fig. 3. The entropy change in natural time under time reversal $\Delta S_i = S_i - (S_-)_i$ for window lengths $i = 3$ to 15 years (left scale) sliding each time by one year through the whole time series from 1979 to 2009. The data (right scale) are depicted by the black points.

Natural time: Eddy heat flux at 10hPa, 1979-2010



The entropy change in natural time under time reversal for various window lengths $i = 3-15$ years sliding each time by one year through the whole time series of eddy heat flux (at 10 hPa) from 1979 to 2010.

Conclusions

- Present status: Significant progress has been achieved in studying the climate variability and the consequences of its changes.

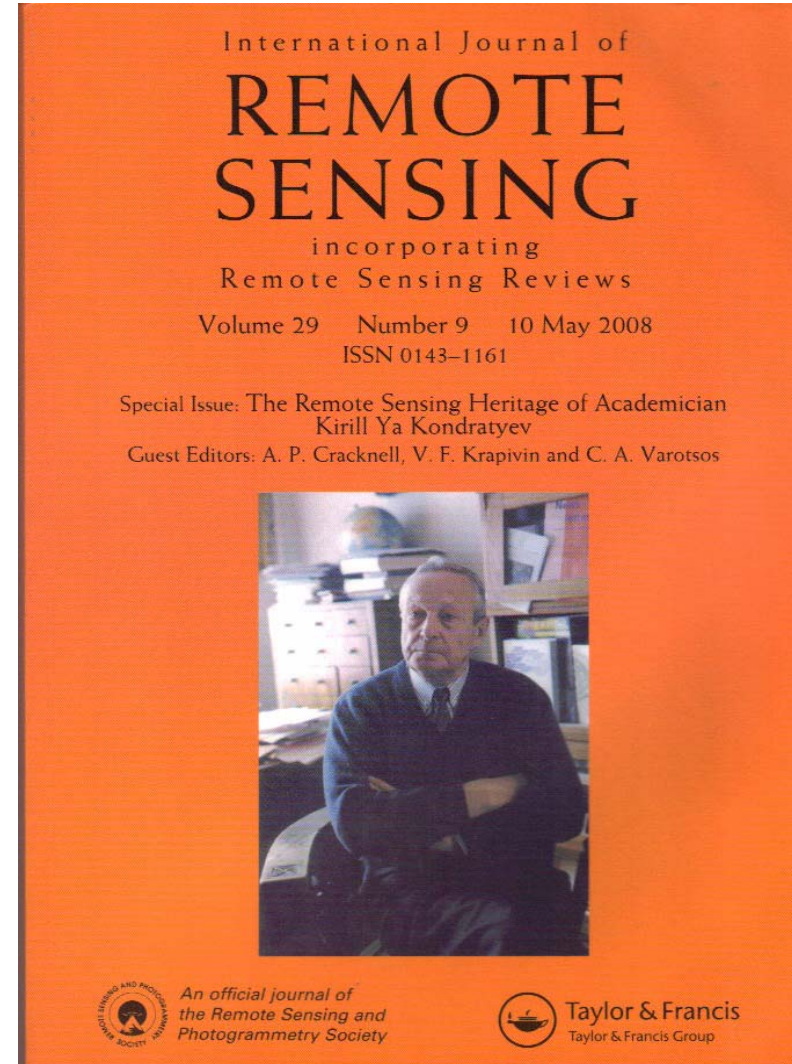
However, a number of related problems remain unsolved so far.

- Future perspectives: There is a necessity for a more comprehensive and integrative consideration of all problems of climate physico-chemistry in their full complexity, taking also into account the long-memory effect that the climate system displays. In order to reduce the level of existing uncertainties in climate forecasts, the improved modelling of atmosphere ocean-land surface-cryosphere-biosphere interactions is urgently required with long-term, non-linear changes in the climate system taken into account.

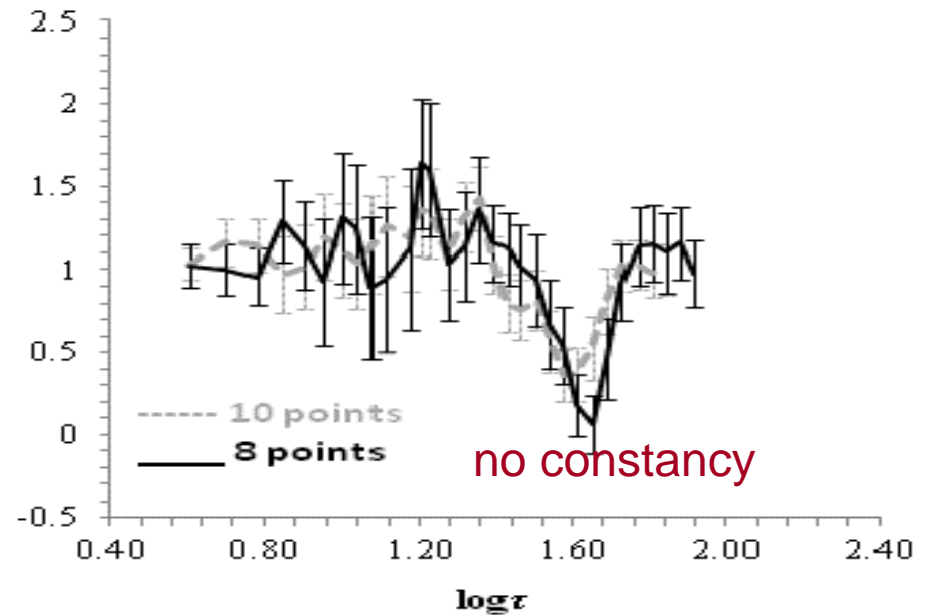
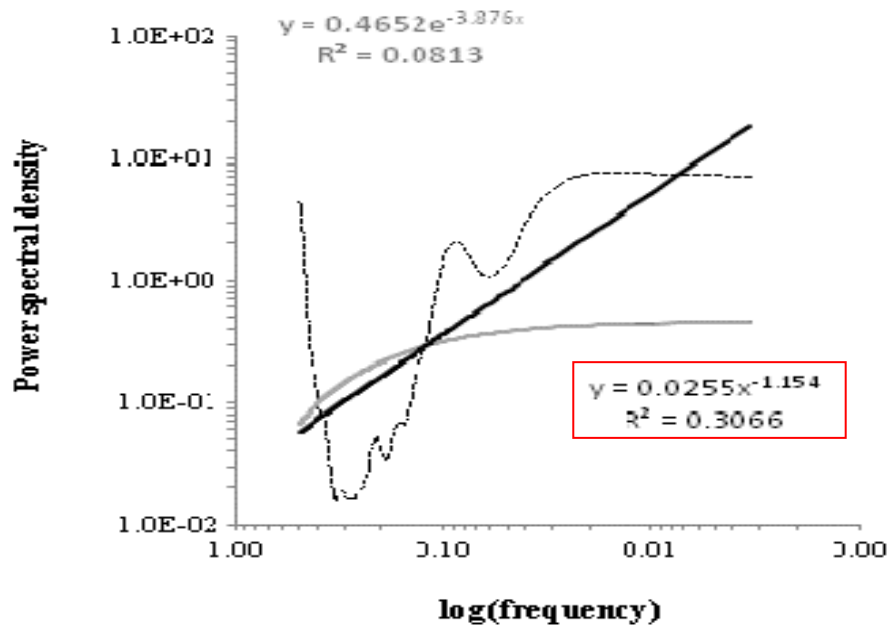
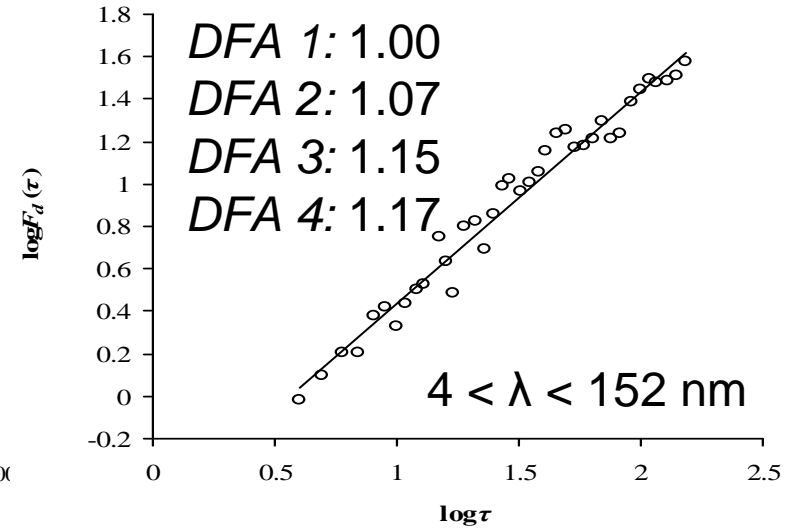
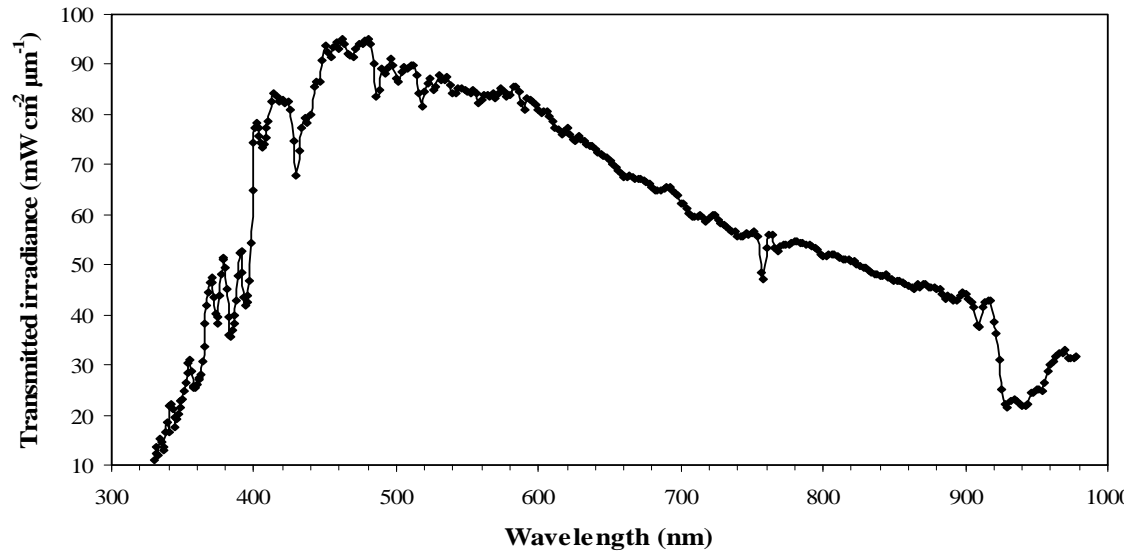
On this basis the remotely sensed data could contribute much to the deeper understanding of the spatio-temporal climate change.



Dedicated to my teacher:
Academician Prof.
Kirill Ya. Kondratyev



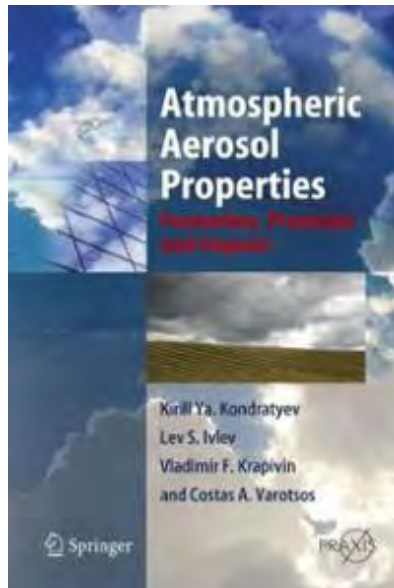
60:38N, 31:36E Local Time 14:35
14.05.1984, The Ladoga Lake, water, Altitude 0.5 Km



Attention: False conclusions about the existence of long-range correlations: a counterexample

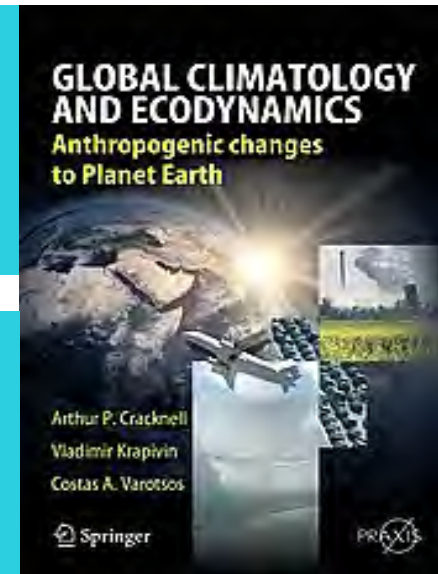
The case of the solar and volcanic forcing over the Tropical Pacific

On the wrong inference of long range correlations in climate data; the case of the solar and volcanic forcing over the Tropical Pacific by *C. Varotsos, M. Efstathiou, Comptes rendus Geoscience, 2013*

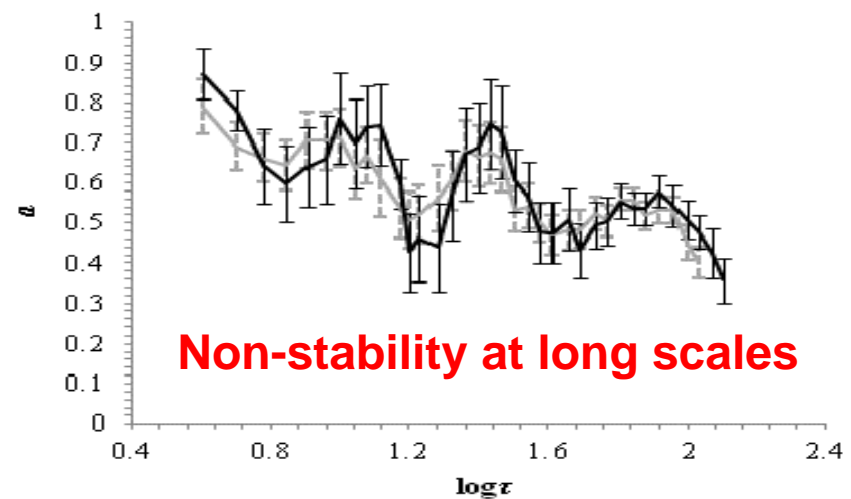
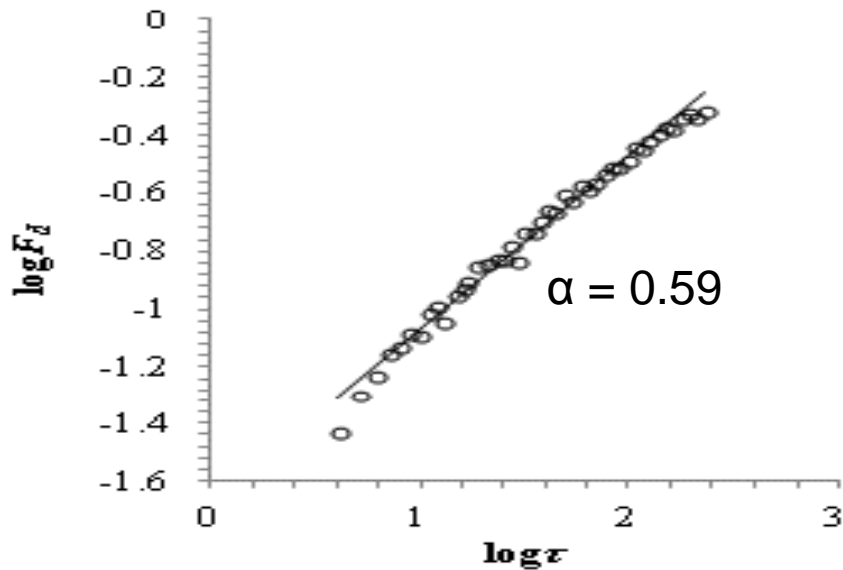
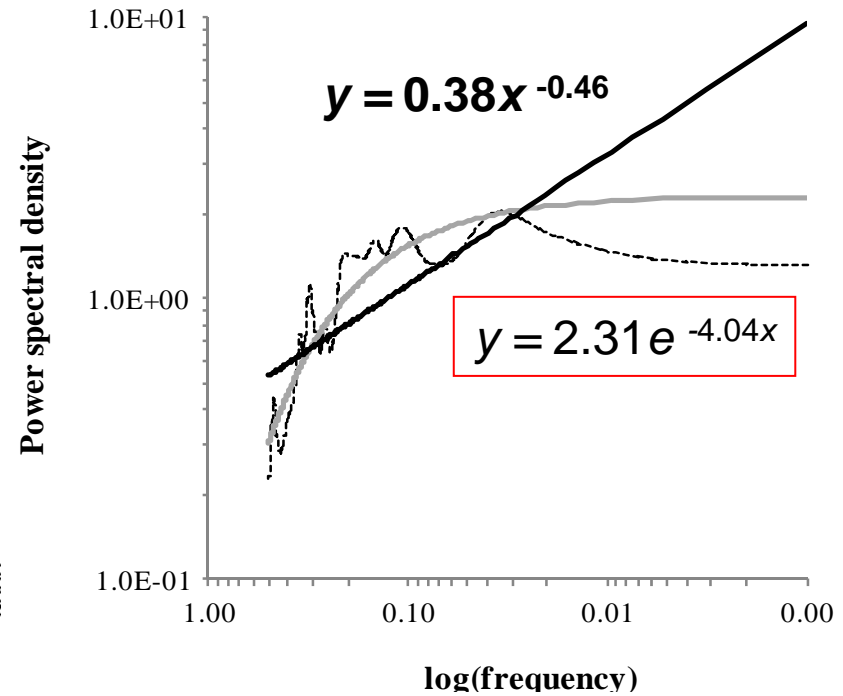
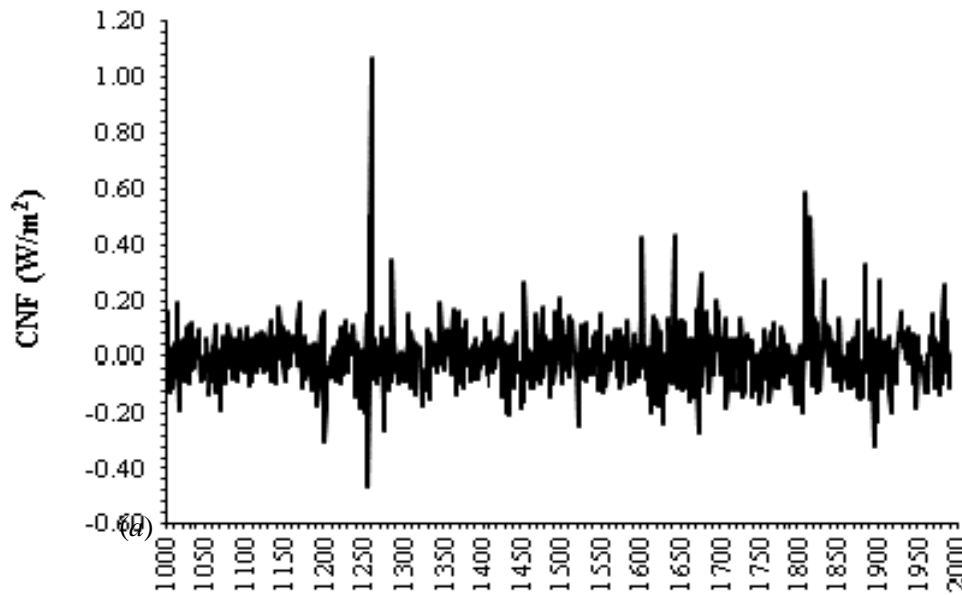


ATMOSPHERIC AEROSOL PROPERTIES: Formation Processes, and Impacts
K. Kondratyev, L. Ivlev, V. Krapivin, C. Varotsos, SPRINGER 608 pages, 2005.

Global Climatology and Ecodynamics: Anthropogenic Changes to Planet Earth
A.P. Cracknell, V. Krapivin. C. Varotsos, SPRINGER, 2008.



1. The combined (solar + volcanic) natural forcing (CNF) during 1000-1999



2. Empirical values of the solar and volcanic forcing

